methylation in chronic hepatitis and cirrhosis—A comprehensive study of loss of heterozygosity and microsatellite instability at 39 loci and DNA hypermethylation on 8 CpG islands in microdissected specimens from patients with hepatocellular carcinoma. *Hepatology.* 2000;32:970-979.

35. Shen L, Kondo Y, Rosner GL, et al. MGMT promoter methylation and field defect in sporadic colorectal cancer. *J Natl Cancer Inst.* 2005;97:1330-1338.
36. Yan PS, Venkataramu C, Ibrahim A, et al. Mapping geographic zones of cancer risk with epigenetic biomarkers in normal breast tissue. *Clin Cancer Res.* 2006;12:6626-6636.
37. Arai E, Kanai Y, Ushijima S, Fujimoto H, Mukai K, Hirohashi S. Regional DNA hypermethylation and DNA methyltransferase (DNMT) 1 protein overexpression in both renal tumors and corresponding nontumorous renal tissues. *Int J Cancer.* 2006;119:288-296.
38. Nakajima T, Yamashita S, Maekita T, Niwa T, Nakazawa K, Ushijima T. The presence of a methylation fingerprint of *Helicobacter pylori* infection in human gastric mucosae. *Int J Cancer.* 2009;124:905-910.
39. Ushijima T, Okochi-Takada E. Aberrant methylations in cancer cells: where do they come from? *Cancer Sci.* 2005;96:206-211.
40. Issa JP, Ahuja N, Toyota M, Bronner MP, Brentnall TA. Accelerated age-related CpG island methylation in ulcerative colitis. *Cancer Res.* 2001;61:3573-3577.
41. van der Vaart H, Postma DS, Timens W, ten Hacken NH. Acute effects of cigarette smoke on inflammation and oxidative stress: a review. *Thorax.* 2004;59:713-721.
42. Wolff EM, Liang G, Cortez CC, et al. RUNX3 methylation reveals that bladder tumors are older in patients with a history of smoking. *Cancer Res.* 2008;68:6208-6214.
43. Garro AJ, McBeth DL, Lima V, Lieber CS. Ethanol consumption inhibits fetal DNA methylation in mice: implications for the fetal alcohol syndrome. *Alcohol Clin Exp Res.* 1991;15:395-398.
44. Choi SW, Stickel F, Baik HW, Kim YI, Seitz HK, Mason JB. Chronic alcohol consumption induces genomic but not p53-specific DNA hypomethylation in rat colon. *J Nutr.* 1999;129:1945-1950.
45. Herceg Z. Epigenetics and cancer: towards an evaluation of the impact of environmental and dietary factors. *Mutagenesis.* 2007;22:91-103.
46. Ushijima T, Nakajima T, Maekita T. DNA methylation as a marker for the past and future. *J Gastroenterol.* 2006; 41:401-407.
47. Graff JR, Gabrielson E, Fujii H, Baylin SB, Herman JG. Methylation patterns of the E-cadherin 5′ CpG island are unstable and reflect the dynamic, heterogeneous loss of E-cadherin expression during metastatic progression. *J Biol Chem.* 2000;275:2727-2732.
48. Shames DS, Minna JD, Gazdar AF. Methods for detecting DNA methylation in tumors: from bench to bedside. *Cancer Lett.* 2007;251:187-198.
49. Hu M, Yao J, Cai L, et al. Distinct epigenetic changes in the stromal cells of breast cancers. *Nat Genet.* 2005;37: 899-905.

Int. J. Cancer: **124,** 2367–2374 (2009)

DNA methylation of microRNA genes in gastric mucosae of gastric cancer patients: Its possible involvement in the formation of epigenetic field defect

Takayuki Ando[1,2], Takeichi Yoshida[1,3], Shotaro Enomoto[3], Kiyoshi Asada[1], Masae Tatematsu[4], Masao Ichinose[3], Toshiro Sugiyama[2] and Toshikazu Ushijima[1]*

[1]*Carcinogenesis Division, National Cancer Center Research Institute, Chuo-ku, Tokyo, Japan*
[2]*Third Department of Internal Medicine, Toyama University, Toyama, Japan*
[3]*Second Department of Internal Medicine, Wakayama Medical University, Wakayama, Japan*
[4]*Division of Oncological Pathology, Aichi Cancer Center Research Institute, Chikusa, Nagoya, Japan*

Accumulation of aberrant DNA methylation in normal-appearing gastric mucosae, mostly induced by *H. pylori* infection, is now known to be deeply involved in predisposition to gastric cancers (epigenetic field defect), and silencing of protein-coding genes has been analyzed so far. In this study, we aimed to clarify the involvement of microRNA (miRNA) gene silencing in the field defect. First, we selected three miRNA genes as methylation-silenced after analysis of six candidate "methylation-silenced" tumor-suppressor miRNA genes. Methylation levels of the three genes (*miR-124a-1, miR-124a-2* and *miR-124a-3*) were quantified in 56 normal gastric mucosae of healthy volunteers (28 volunteers with *H. pylori* and 28 without), 45 noncancerous gastric mucosae of gastric cancer patients (29 patients with *H. pylori* and 16 without), and 28 gastric cancer tissues (13 intestinal and 15 diffuse types). Among the healthy volunteers, individuals with *H. pylori* had 7.8–13.1-fold higher methylation levels than those without ($p < 0.001$). Among individuals without *H. pylori*, noncancerous gastric mucosae of gastric cancer patients had 7.2–15.5-fold higher methylation levels than gastric mucosae of healthy volunteers ($p < 0.005$). Different from protein-coding genes, individuals with past *H. pylori* infection retained similar methylation levels to those with current infection. In cancer tissues, methylation levels were highly variable, and no difference was observed between intestinal and diffuse histological types. This strongly indicated that methylation-silencing of miRNA genes, in addition to that of protein-coding genes, contributed to the formation of a field defect for gastric cancers.

Key words: field for cancerization; microRNA; methylation; gastric cancer; *Helicobacter pylori*

Metachronous occurrence of gastric cancers is becoming an important issue as localized resection of early gastric cancers by endoscopic submucosal dissection (ESD) has become common.[1] The incidence of secondary primary gastric cancers after ESD reaches as high as 2.0% per year[2] whereas the incidence of gastric cancer in the general Japanese population is 0.14% per year.[3] This indicates that noncancerous gastric mucosae are already predisposed to developing gastric cancers, forming a field defect (field for cancerization). High incidences of metachronous cancers have been known not only for gastric cancers but also for bladder, liver, and esophageal cancers[4–6] and are becoming recognized for lung, breast and colorectal cancers.[7–9]

A molecular basis for the field defect has been considered as an accumulation of genetic and epigenetic alterations in normal-appearing tissues. Traditionally, cells with a genetic alteration were considered to form a physically continuous patch, producing a genetically altered field.[10] Recently, we found that aberrant DNA methylation of specific genes can be induced in as high as several percentage of cells in noncancerous gastric mucosae (thus in multiple independent gastric glands), and the degree of methylation is associated with gastric cancer risks.[11,12] Importantly, *Helicobacter pylori* infection, a major carcinogenic factor in the stomach, was shown to potently induce aberrant DNA methylation in gastric epithelial cells.[11] In addition to gastric cancers, the presence of aberrant DNA methylation in noncancerous tissues and possible association with cancer risks have been reported for liver,[13] colon,[14] esophageal,[15] breast[16] and renal cancers.[17]

Genes so far analyzed in noncancerous gastric mucosae are those methylated in gastric cancers, including tumor-suppressor genes, such as *CDKN2A, MLH1, CDH1, LOX* and *APC*,[2,11,18,19] and genes with little or no expression in normal gastric mucosae, such as *FLNc, HAND1* and *THBD*. The latter group of genes is methylated in parallel with tumor-suppressor genes but with higher frequencies, and is considered as a good marker to detect the presence of an epigenetic field defect.[11] In contrast with these protein-coding genes, involvement of microRNA (miRNA) silencing in field defect formation has not been clarified yet. Since the role of aberrant expression or reduction of various miRNAs in human multistep carcinogenesis is now clear,[20,21] there is a possibility that miRNAs silencing by aberrant DNA methylation is involved in field defect formation. Indeed, several tumor-suppressor miRNAs, including *miR-124a*,[22] *miR-137*, *miR-193a*[23] and *miR-127*,[24] are reported to be silenced by aberrant DNA methylation of their promoter CpG islands (CGI) in cancers.

In this study, we aimed to clarify whether or not miRNA silencing by DNA methylation can be involved in the formation of a field defect for gastric cancers. First, we searched for miRNAs that are reported to have tumor-suppressive functions and be controlled by DNA methylation, and confirmed methylation-silencing of these candidate genes. Then, we quantified their methylation levels in gastric mucosae of healthy volunteers, noncancerous gastric mucosae of gastric cancer patients, and primary gastric cancer tissues.

Material and methods

Cell lines and tissue samples

Six gastric cancer cell lines, AGS, KATOIII, MKN28, MKN45, MKN74 and NUGC3 were obtained from the Japanese Collection of Research Bioresources (Tokyo, Japan) and the American Type Culture Collection (Manassas, VA). Three gastric cancer cell lines, HSC39, HSC44 and HSC57 were gifted by Dr. K. Yanagihara, National Cancer Center Research Institute, Tokyo, Japan. GC2 was developed by M. T. TMK1 was gifted by Dr. W. Yasui, Hiroshima University, Hiroshima, Japan. 5-Aza-2′-deoxycitidine (5-aza-dC) treatment was performed with AGS, HSC57 and MKN28. Cells were seeded on day 0, media was added with freshly prepared 5-aza-dC on days 1 and 3, and cells were harvested on day 5. The concentrations of 5-aza-dC were determined as minimum concentrations that deplete DNMT1.[25]

Gastric mucosae were obtained by endoscopic biopsy of antral regions from 56 healthy volunteers (25 male and 31 female; aver-

Additional Supporting Information may be found in the online version of this article.

Grant sponsor: Ministry of Health, Labour and Welfare, Japan.

***Correspondence to:** Carcinogenesis Division, National Cancer Center Research Institute, 5-1-1 Tsukiji, Chuo-ku, Tokyo, Japan.
Fax: +81-3-5565-1753. E-mail: tushijim@ncc.go.jp

Received 5 August 2008; Accepted after revision 25 November 2008
DOI 10.1002/ijc.24219
Published online 11 December 2008 in Wiley InterScience (www.interscience.wiley.com).

age age 53, ranging from 27 to 91) and 45 gastric cancer patients (35 male and 10 female; average age 66, ranging from 38 to 89). Gastric cancer tissues were obtained from 28 gastric cancer patients (21 male and 7 female; average age 66, ranging from 49 to 81; 13 intestinal and 15 diffuse types) who underwent gastrectomy due to gastric cancers. Gastric epithelial cells were obtained by the gland isolation technique from eight noncancerous gastric tissues. Informed consents were obtained from all the patients and healthy volunteers. Gastric mucosae, noncancerous mucosae and cancer tissues were frozen in liquid nitrogen immediately after biopsy or resection, and stored at −80°C until extraction of genomic DNA. High molecular weight DNA was extracted by the phenol/chloroform method. RNA was isolated with ISOGEN (Nippon Gene, Tokyo, Japan).

H. pylori infection status was analyzed by a serum anti-*H. pylori* IgG antibody test (SRL, Tokyo, Japan), rapid urease test (Otsuka, Tokushima, Japan), or culture test (Eiken, Tokyo, Japan). All cancers were histologically diagnosed according to the Japanese classification of gastric carcinoma,[26] and classified according to the Lauren classification system.[27]

Sodium bisulfite modification, methylation-specific PCR (MSP), quantitative real-time MSP and bisulfite sequencing

Fully methylated DNA and fully unmethylated DNA were prepared by methylating genomic DNA with *Sss*I methylase (New England Biolabs, Beverly, MA) and by amplifying genomic DNA with the GenomiPhi amplification system (GE Healthcare, Buckinghamshire, UK), respectively. Bisulfite modification was performed using 1 μg of *Bam*HI-digested genomic DNA as previously described,[28] and the modified DNA was suspended in 40 μl of Tris-EDTA buffer. An aliquot of 1 μl was used for methylation-specific PCR (MSP) and Quantitative real-time MSP (qMSP) with a primer set specific to methylated (M) or unmethylated (U) sequences.

For MSP, the fully methylated and unmethylated DNA was used to determine an annealing temperature that specifically amplifies only methylated or unmethylated DNA. A minimum number of PCR cycles to obtain visible bands was determined using the fully (un)methylated DNA, and four cycles were added for analysis of gastric cancer cell lines. The primers were designed just upstream of reported transcription start sites within the CGI (Table I; Fig. 1*a*), whose methylation statuses are now known to be critical for induction of gene silencing.[29,30]

qMSP was performed by real-time PCR using SYBR® Green I (BioWhittaker Molecular Applications, Rockland, ME) and an iCycler Thermal Cycler (Bio-Rad Laboratories, Hercules, CA). Although the same primer set was used for qMSP, a specific annealing temperature in the presence of SYBR® Green I was redetermined using the fully methylated and unmethylated DNA. The number of molecules in a sample was determined by comparing its amplification with those of standard DNA that contained exact numbers of molecules (10^1–10^6 molecules). Based on the numbers of M molecules and U molecules for a genomic region, a methylation level of the region was calculated as the fraction of M molecules in the total number of DNA molecules (# of M molecules + # of U molecules). The standard DNA samples were prepared by cloning PCR products of methylated and unmethylated sequences into the pGEM-T Easy vector (Promega, Madison, WI), respectively, or by purifying the PCR products using the Wizard SV Gel and PCR clean-up system (Promega).

For bisulfite sequencing, an aliquot of 1 μl of the sodium bisulfite-treated DNA was amplified by PCR with the primers common to methylated and unmethylated DNA sequences (Table I). The PCR product was cloned into pGEM-T Easy vector (Promega), and 15 clones or more were cycle-sequenced for each sample.

Quantitative real-time reverse transcription (RT)-PCR

For quantitative RT-PCR, cDNA was synthesized from 10 ng of total RNA using TaqMan® MicroRNA-specific primers and a

TABLE I – PRIMERS AND CONDITIONS FOR MSP AND REAL-TIME MSP

Gene	M/U	Primer sequence		Length (bp)	Annealing (°C)		Number of cycles for MSP
		Forward (5′→3′)	Reverse (5′→3′)		MSP	Real-time MSP	
miR-124a-1	M	AGAGTTTTGGAAGACGTCG	AAAAAATATAAAAACGACGC	155	58	58	36
	U	AATAAAGAGTTTTGGAAGATGTT	CAAAAA AAA AAAATAAAAACAACAC	166	58	58	36
miR-124a-2	M	GGTTTATGTATGTTTTTAGGCG	TCCGTAAAATATAAACGATAG	93	59	56	32
	U	TAGGTTTATGTATGTTTTTAGGTG	CTATTCCATAAAAATATAAACAATACA	99	52	50	36
miR-124a-3	M	GATAGTATAGTCGGTTGAGCGTAGC	CCTCAAACTAAAACGAACGACG	152	61	59	31
	U	TAGTTGGTTGAGTGTAGTGTTTTTG	CAAACTAAAACAAACAACAAACATC	142	61	59	36
miR-137	M	TAGGGCGGGTTAGCG	TACCGCTACCGCTACTACC	99	57	–	36
	U	TTTTGGTGGTGGTTGGTGGT	ACCCAAAAATACCATCACCA	113	63	–	35
miR-193a	M	GAGGTAGTTTGGTCGGAGCGTAC	GACCCCCGAAACCAACG	86	61	–	36
	U	ATTGATTTATATTTTTGAGAGTGTTG	TCCCAAACTAACATACACTCCA	153	58	–	35
miR-127	M	GTTTGGGGAGAGCGTAAACG	GTAAACGAACACCGCACCG	96	63	–	34
	U	GTTTTGTGAATTATTTGGTTTTG	TTACAAATATCCCTCCACCAC	176	58	–	38

Gene	Primers for bisulfite sequencing		Length (bp)	Annealing (°C)	Number of cycles
	Forward (5′→3′)	Reverse (5′→3′)			
miR-124a-1	AAGGATGGGGGAGAATAAAGAGTTT	CTCAACCAACCCCATTCTTAACATT	354	60	32
miR-124a-2	ATTAGATTTATAGGTTTATGTATGTTTTTAGG	ACTCTTCTCTCCCTACCCATC	235	54	30
miR-124a-3	GAAAGGGGAGAAGTGTGGGTTTTT	CTCTTAACATTCACCGCGTACCTTAAT	268	54	32

M, Primers specific to methylated DNA; U, Primers specific to unmethylated DNA.

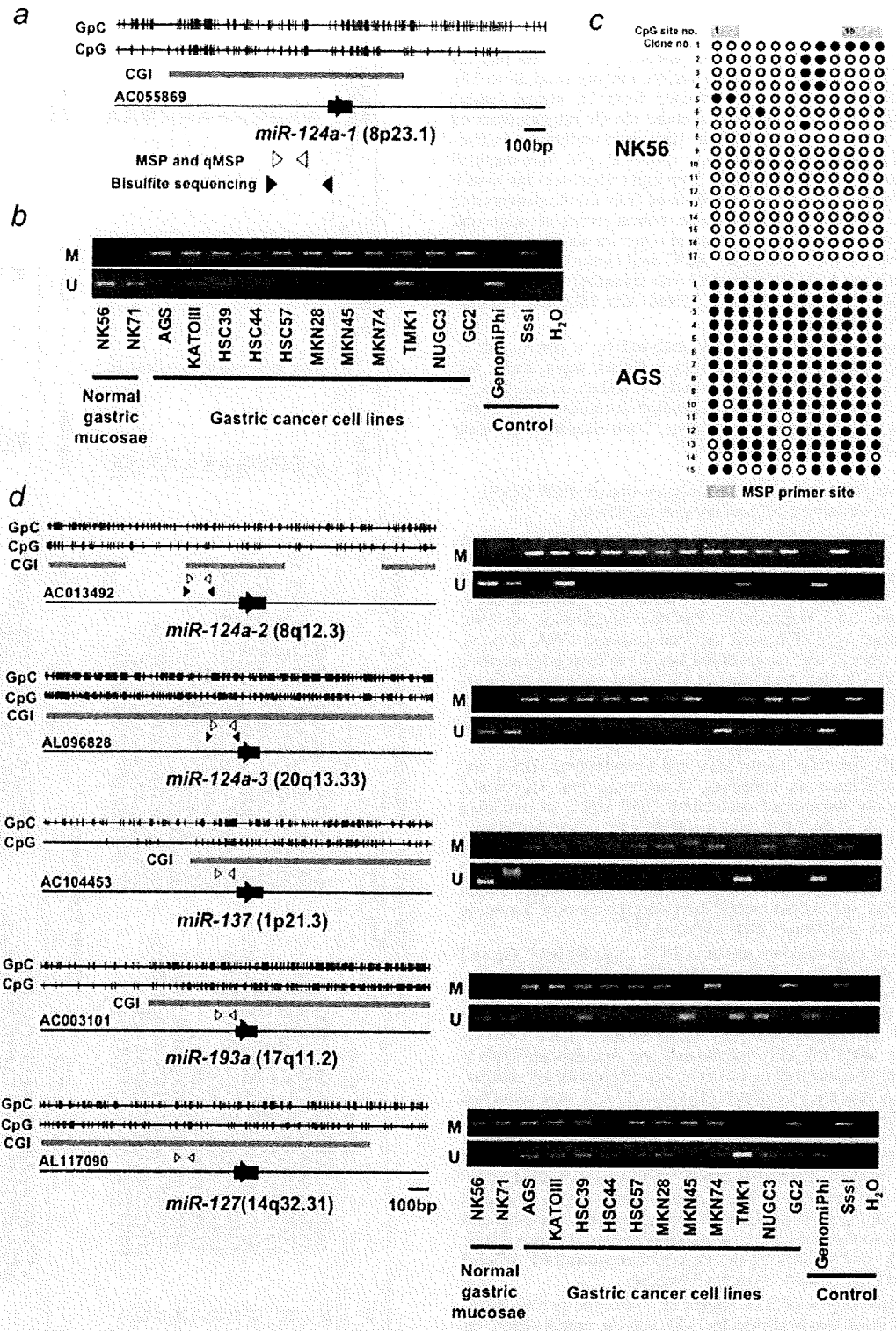

FIGURE 1 – Genomic structures and methylation statuses of the six miRNA genes in gastric cancer cell lines. (*a*) Structures of the *miR-124a-1* gene. Vertical ticks, individual GpC (top) and CpG sites (bottom); gray box, CGI; closed box, genomic location of *miR-124a-1*; open arrowheads, locations of the primers for MSP and real-time MSP; and closed arrowheads, locations of the primers for bisulfite sequencing. (*b*) Methylation statuses of *miR-124a-1* in normal gastric mucosae and 11 gastric cancer cell lines analyzed by MSP. SssI, genomic DNA methylated by *SssI* methylase; GenomiPhi, genomic DNA amplified by GenomiPhi; and M and U, primer sets specific to methylated and unmethylated DNA, respectively. (*c*) The methylation status of a CGI around *miR-124a-1* analyzed by bisulfite sequencing. Twelve CpG sites were analyzed in NK56 normal and AGS gastric cancer cell lines, and 15 clones or more were sequenced for each sample. Closed circle, methylated CpG site; and open circle, unmethylated CpG site. (*d*) Genomic structures of five other miRNA genes and their methylation statuses in normal gastric mucosae and 11 gastric cancer cell lines analyzed by MSP.

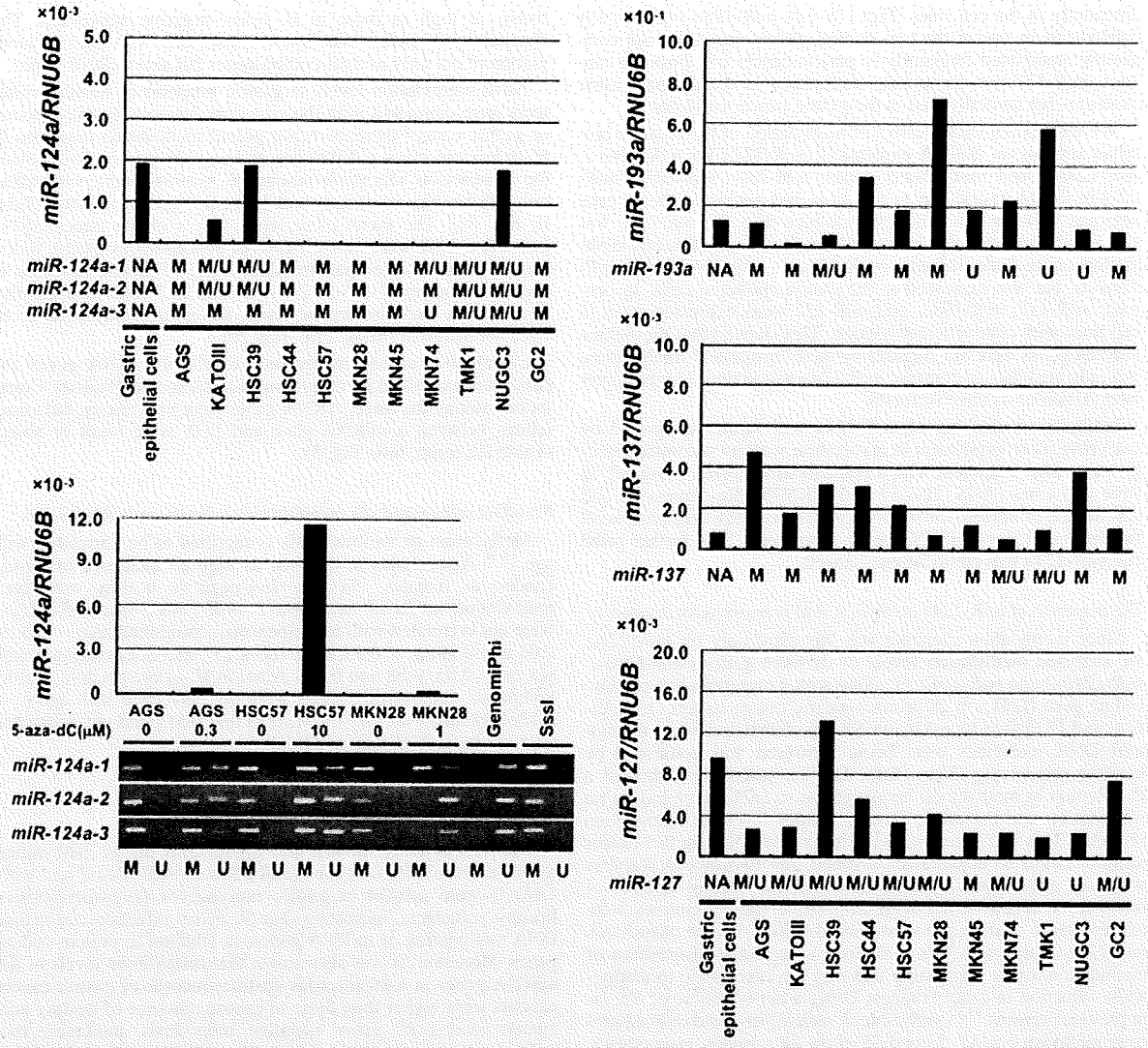

FIGURE 2 – Expression levels of miRNAs in gastric epithelial cells and gastric cancer cell lines. Expression levels were analyzed by quantitative RT-PCR, and normalized to *RNU6B* expression. Gastric epithelial cells were obtained by gland isolation technique from noncancerous tissues of eight gastric cancer patients, and average expression levels of the eight patient samples are shown. Results of MSP were duplicated from Figure 1 for convenience. M, M/U and U represent the presence of only methylated DNA, both methylated and unmethylated DNA, and only unmethylated DNA, respectively. NA, not applicable. Only *miR-124a* showed consistent repression in cell lines without unmethylated DNA molecules. After treatment by 5-aza-dC, *miR-124a* was re-expressed abundantly in HSC57, in association with demethylation, and in AGS and MKN28.

TaqMan® MicroRNA Reverse Transcription Kit (Applied Biosystems, Foster City, CA). Real-time PCR was performed using the ABI Prism 7300 Fast Real-Time PCR System (Applied Biosystems). Expression levels of target miRNAs were normalized to that of a small nuclear RNA *RNU6B* transcript.

Statistical analysis

A difference in mean methylation levels was analyzed by the *t*-test Welch method, and differences in methylation incidence in gastric cancer tissues were analyzed by the chi-square test. Correlation between the age and methylation levels of miRNA genes, and correlation between methylation levels of each gene were analyzed using Spearman's rank correlation coefficient. All the analyses were performed using SPSS (SPSS, Inc., Chicago, IL), and the results were considered significant when a p value less than 0.05 was obtained by two-sided tests.

Results

Identification of miRNAs silenced in gastric cancer cell lines

Six genes of four miRNAs (*miR-124a, miR-137, miR-193a* and *miR-127*) were reported to have a tumor-suppressive function and be controlled by DNA methylation in colon, bladder and oral cancers.[22–24] We first analyzed methylation statuses of their putative promoter regions in 11 gastric cancer cell lines and two normal gastric mucosae of healthy individuals without *H. pylori*. It was found that *miR-124a-1, miR-124a-2, miR-124a-3* and *miR-137* were unmethylated in the normal gastric mucosae, but were completely methylated (no unmethylated DNA molecules detected)

frequently in the cell lines (Figs. 1*b*–1*d*). *miR-193a* was partially methylated in one of the two normal gastric mucosae, and completely methylated frequently in gastric cancer cell lines. In contrast, *miR-127* was completely methylated in the normal gastric mucosae, but unmethylated in the gastric cancer cell lines.

We then examined the effect of methylation of the putative promoter regions on miRNA expression (*miR-124a* for *miR-124a-1*, *miR-124a-2* and *miR-124a-3* genes; *miR-137*; *miR-193a*; *miR-127*) in the 11 gastric cancer cell lines and gastric epithelial cells obtained by the gland isolation technique (Fig. 2). *miR-124a* was consistently unexpressed in six cell lines with simultaneous methylation of its three isoforms (*miR-124a-1*, *miR-124a-2* and *miR-124a-3*), but was expressed in the gastric epithelial cells. In contrast, *miR-137*, *miR-193a*, and *miR-127* were expressed even in cell lines with complete methylation. This showed that these three miRNA genes were not silenced by their "promoter" methylation, and indicated that, in contrast, *miR-124a* was silenced by promoter methylation of its three isoforms.

Methylation-silencing of *miR-124a* was further confirmed by analyzing its re-expression in association with its promoter demethylation after treatment with a demethylating agent, 5-aza-dC, in three cell lines (AGS, HSC57 and MKN28). Re-expression and appearance of unmethylated DNA molecules were observed in all the three cell lines, HSC57 being prominent. This further orted that *miR-124a* was methylation-silenced.

The presence of miR-124a *methylation in primary gastric cancers*

Since methylation-silencing was identified only for *miR-124a*, we analyzed methylation levels of its three genes (*miR-124a-1*, *miR-124a-2* and *miR-124a-3*), along with a representative protein-coding gene (*LOX*), in 28 primary gastric cancer tissues (13 intestinal and 15 diffuse types) by qMSP. The fact that densely methylated DNA molecules were being measured was confirmed by bisulfite sequencing (Supp. Info. Fig. 1). *miR-124a-1* showed a distribution of methylation levels similar to *LOX*, some having no methylation and the others having various levels of methylation (Fig. 3*a*). This was consistent with our previous finding that cancer samples could be essentially classified into two groups (cancers with and without methylation), and that the various degrees of methylation levels in methylation-positive cancer samples were mainly due to contamination of normal cells.[18] On the other hand, *miR-124a-2* and *miR-124a-3* showed a unimodal distribution of methylation levels, suggesting that they are susceptible to methylation induction in cancer tissues. Using a cut-off value of 6%, as in previous reports,[31,32] *miR-124a-1*, *miR-124a-2* and *miR-124a-3* were methylated in 11, 23 and 26 of the 28 samples, respectively. Between the two histological types, the incidences of methylation were the same for *miR-124a-1*, *miR-124a-2* and *miR-124a-3* (p = 0.95, 0.84 and 0.67) (Supp. Info. Fig. 2a).

We further analyzed an association between methylation and expression of *miR-124a* in an additional 19 gastric cancer samples. Using a cut-off value of 6%, eight samples had methylation of all the three *miR-124a* genes, and the other 11 samples had methylation of only one or two genes and retained at least one unmethylated gene. *miR-124a* was barely expressed in all the eight samples with methylation of the three genes whereas it was expressed in 5 of 11 cancer samples with at least one unmethylated gene (Fig. 3*b*).

Accumulation of methylation in H. pylori *positive gastric mucosae, and its association with gastric cancer risk*

Methylation levels of *miR-124a-1*, *miR-124a-2* and *miR-124a-3*, again along with *LOX*, were analyzed by qMSP in gastric mucosae of 56 healthy volunteers (28 volunteers with *H. pylori* and 28 without) and noncancerous gastric mucosae of 45 gastric cancer patients (29 patients with *H. pylori* and 16 without) (Fig. 3*b*). Among the healthy volunteers, the mean methylation levels of *miR-124a-1*, *miR-124a-2*, *miR-124a-3* and *LOX* in the *H. pylori*-positive individuals were 13.1-, 7.8-, 8.9- and 46.7-fold, respectively, as high as those in *H. pylori*-negative individuals. This showed that *H. pylori* infection was associated with aberrant methylation of not only protein-coding genes but also miRNA genes.

Next, methylation levels in gastric mucosae of healthy volunteers were compared with those of noncancerous gastric mucosae of gastric cancer patients. Since potent methylation induction by *H. pylori* can mask a difference in *H. pylori*-positive individuals, the comparison was made among *H. pylori*-negative individuals only (28 healthy volunteers and 16 gastric cancer patients) (Table II; Fig. 3*c*). The mean methylation levels of the three miRNA genes and *LOX* were much higher in noncancerous gastric mucosae of gastric cancer patients than those of gastric mucosae of healthy volunteers (15.5-, 7.2-, 13.3- and 24.7-fold, respectively). Between the two histological types, the mean methylation levels were not different (Supp. Info. Fig. 2b).

Correlations among methylation levels of miRNA genes and *LOX* were examined by calculating correlation coefficients. Correlations among the three miRNA genes were very strong, but correlations between a miRNA gene and *LOX* were weak or absent (Table III; Supp. Info. Fig. 3).

No effect of age and sex on methylation levels on miRNA genes

Methylation of various CGIs is reported to be correlated with age.[33,34] Also, males have twice as high an incidence of gastric cancers as females.[1] In *H. pylori*-negative healthy volunteers, methylation levels of *miR-124a-1, miR-124a-2 and miR-124a-3* were not correlated with age (Spearman correlation test: r = 0.19, 0.01 and 0.29; p = 0.35, 0.94 and 0.15), and not associated with sex (p = 0.05, 0.68 and 0.19). Also, in *H. pylori*-positive healthy volunteers, methylation levels were not correlated with age (r = 0.13, 0.18 and −0.1; p = 0.51, 0.35 and 0.51), and not associated with sex (p = 0.70, 0.20 and 0.67).

Discussion

The present study showed that significantly higher methylation levels of three miRNA genes (*miR-124a-1, miR-124a-2* and *miR-124a-3*) were present in gastric mucosae of *H. pylori*-positive healthy volunteers, indicating that *H. pylori* infection can induce DNA methylation of miRNA genes, in addition to protein-coding genes. Moreover, it was also shown that methylation levels of the miRNA genes in noncancerous gastric mucosae of gastric cancer patients were higher than those in gastric mucosae of healthy volunteers among *H. pylori* negative individuals, indicating that miRNA silencing is involved in the formation of a field defect for gastric cancers. To our knowledge, the presence of miRNA silencing in a field for cancerization was shown here for the first time.

Recent studies demonstrated that expression of some miRNAs is regulated by epigenetic mechanisms.[24,35] From six miRNA genes that were reported to be silenced by promoter methylation and to have tumor-suppressor functions, we were able to confirm that three genes of *miR-124a* were methylation-silenced in gastric cancer cell lines. The other three genes, *miR-137, miR-193a* and *miR-127*, were expressed even in cell lines with complete methylation, and were unlikely to be silenced by promoter methylation in gastric cancers. Since methylation of putative promoter regions consistently represses transcription of their downstream genes,[29,30] the presence of the expression of the three genes in gastric cancer cell lines with complete methylation of their "promoter" CGI indicated that the three genes had additional or alternative promoters.

Lujambio *et al.*[22] discovered that *miR-124a* was silenced by promoter methylation after screening 320 miRNA genes. They also found that *miR-124a* down-regulates CDK6, a demonstrated oncogene involved in cell cycle progression and differentiation, and induces hypophosphorylation of RB.[22] Therefore, it is possible that *miR-124a* silencing is also involved in gastric carcinogenesis, and the presence of its silencing in noncancerous tissues

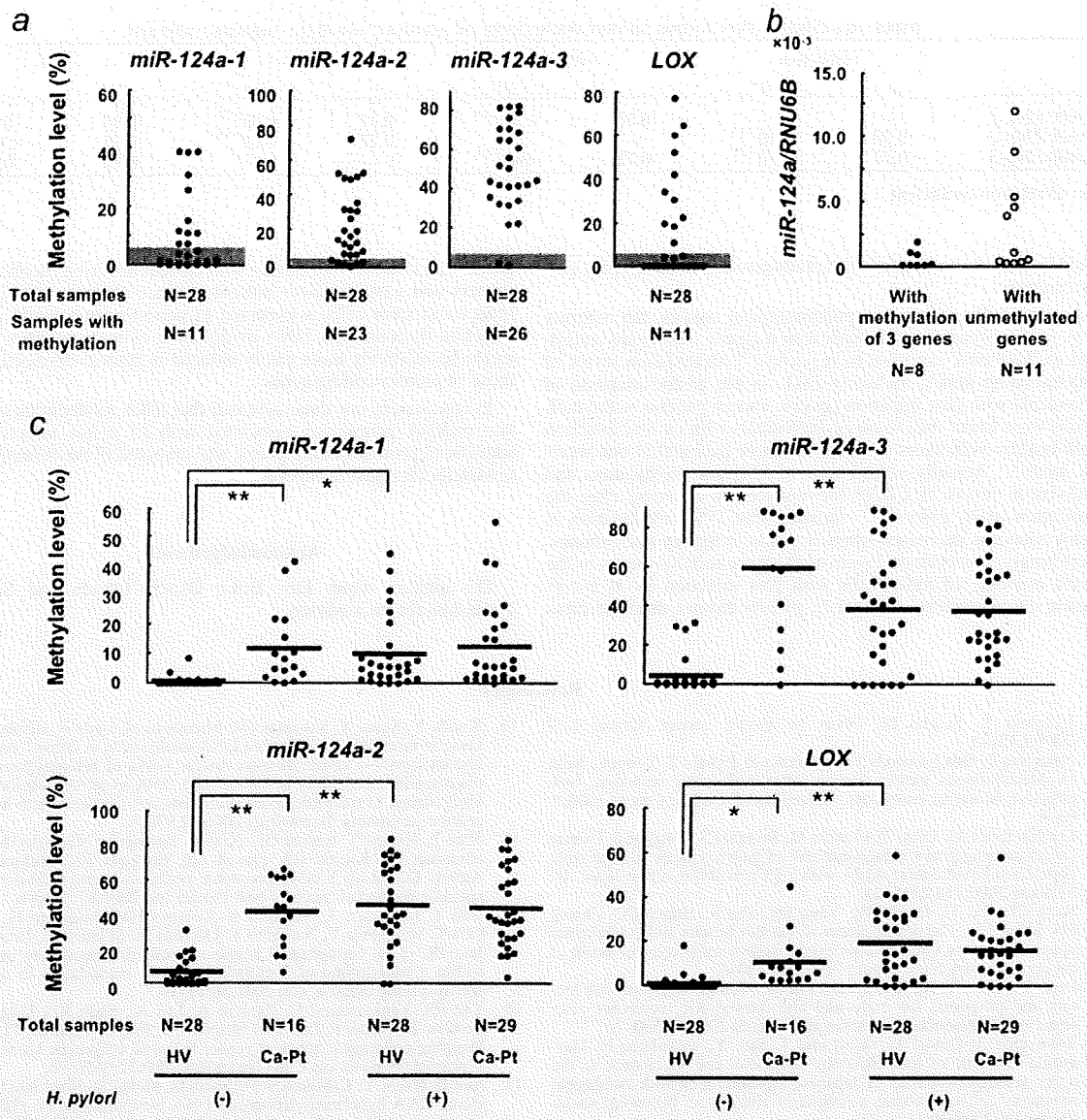

FIGURE 3 – Methylation levels of *miR-124a-1*, *miR-124a-2*, *miR-124a-3* and *LOX* in gastric mucosae of healthy volunteers, noncancerous mucosae of gastric cancer patients, and cancer tissues. (*a*) Distribution of methylation levels in gastric cancers. Gray areas show samples with methylation levels below the cut-off value of 6%. (*b*) Expression of *miR-124a* in eight cancer samples with methylation (three *miR-124a* genes, methylation positive) and 11 cancer samples with at least one unmethylated gene (*miR-124a-1* or *miR124a-3*). Five of the 11 cancers with unmethylated genes had high *miR-124a* expression levels. (*c*) Distribution of methylation levels in gastric mucosae of healthy volunteers (HV) and noncancerous mucosae of gastric cancer patients (Ca-Pt). A horizontal line represents a mean methylation level for each group. Among the healthy volunteers, *H. pylori*-positive individuals had 7.8–46.7-fold as high methylation levels as *H. pylori*-negative individuals (*$p < 0.005$; **$p < 0.001$). Among the *H. pylori*-negative individuals, noncancerous gastric mucosae of gastric cancer patients had 7.2–24.7-fold as high methylation levels as gastric mucosae of healthy volunteers (*$p < 0.005$; **$p < 0.001$).

TABLE II – MEAN METHYLATION LEVELS AND STANDARD DEVIATIONS OF THE FOUR GENES IN GASTRIC MUCOSAE OF HEALTHY VOLUNTEERS AND GASTRIC CANCER PATIENTS

		N	*miR-124a-1*	*miR-124a-2*	*miR-124a-3*	*LOX*
H.pylori(−)	(1) Healthy volunteers	28	0.76 ± 1.70	5.75 ± 7.73	4.45 ± 9.29	0.43 ± 1.22
	(2) Gastric cancer patients	16	11.82 ± 12.94	41.66 ± 19.33	59.42 ± 30.71	10.64 ± 11.33
H.pylori(+)	(3) Healthy volunteers	28	9.96 ± 12.28	44.79 ± 23.96	39.66 ± 30.08	20.10 ± 15.72
	(4) Gastric cancer patients	29	12.28 ± 14.31	46.33 ± 28.36	37.48 ± 25.13	15.93 ± 12.58
p value	(1) *vs.* (3)		<0.001	$<10^{-8}$	$<10^{-5}$	$<10^{-6}$
	(1) *vs.* (2)		0.004	$<10^{-5}$	$<10^{-6}$	0.003
	(3) *vs.* (4)		0.51	0.77	0.77	0.28

TABLE III – CORRELATION AMONG METHYLATION LEVEL OF *miR-124A-1*, *miR-124A-2*, *miR-124A-3* AND *LOX*

	miR-124a-1		*miR-124a-2*		*miR-124a-3*		*LOX*	
	r	*p*	*r*	*p*	*r*	*p*	*r*	*p*
miR-124a-1	–	–	0.70	$<10^{-15}$	0.77	$<10^{-20}$	0.03	0.76
miR-124a-2	0.70	10^{-15}	–	–	0.72	$<10^{-16}$	0.37	$<10^{-3}$
miR-124a-3	0.77	$<10^{-20}$	0.72	$<10^{-16}$	–	–	0.20	0.04

r, correlation coefficient.

could be directly associated with predisposition to developing gastric cancers.

As repeatedly shown by epidemiological studies, the majority of *H. pylori*-negative individuals with a gastric cancer are considered to have past exposure to *H. pylori*.[36] Methylation levels of protein-coding genes, including *LOX*, in the gastric mucosae of individuals with past infection (gastric cancer patients without *H. pylori*) were lower than those of individuals with current infection (both healthy volunteers and gastric cancer patients) in our previous study.[11] Actually, incidences of aberrant methylation and methylation levels of *CDH1* are reported to decrease after the eradication of *H. pylori*,[19,37] showing that DNA methylation in gastric mucosae decreases when *H. pylori* infection discontinues. Interestingly, methylation levels of the three miRNA genes in the gastric mucosae of individuals with past infection by *H. pylori* (gastric cancer patients without *H. pylori*) did not decrease compared with those of individuals with current infection (healthy volunteers and gastric cancer patients). Since aberrant methylation induced in stem cells is expected to persist even after *H. pylori* infection discontinues, DNA methylation of these miRNA genes might be relatively more easily induced in gastric stem cells than those of protein-coding genes.

In conclusion, our data indicated that DNA methylation of certain miRNA genes was associated with *H. pylori* infection, in addition to protein-coding genes, and involved in the formation of field defect for gastric cancers.

Acknowledgements

The authors thank Drs. Eriko Okochi-Takada and Satoshi Yamashita for their advice.

References

1. Ushijima T, Sasako M. Focus on gastric cancer. Cancer Cell 2004;5:121–5.
2. Nakajima T, Oda I, Gotoda T, Hamanaka H, Eguchi T, Yokoi C, Saito D. Metachronous gastric cancers after endoscopic resection: how effective is annual endoscopic surveillance? Gastric Cancer 2006;9: 93–8.
3. Lee KJ, Inoue M, Otani T, Iwasaki M, Sasazuki S, Tsugane S. Gastric cancer screening and subsequent risk of gastric cancer: a large-scale population-based cohort study, with a 13-year follow-up in Japan. Int J Cancer 2006;118:2315–21.
4. Kang CH, Yu TJ, Hsieh HH, Yang JW, Shu K, Huang CC, Chiang PH, Shiue YL. The development of bladder tumors and contralateral upper urinary tract tumors after primary transitional cell carcinoma of the upper urinary tract. Cancer 2003;98:1620–6.
5. Poon RT, Fan ST, Ng IO, Lo CM, Liu CL, Wong J. Different risk factors and prognosis for early and late intrahepatic recurrence after resection of hepatocellular carcinoma. Cancer 2000;89:500–7.
6. Yokoyama A, Omori T, Yokoyama T, Sato Y, Kawakubo H, Maruyama K. Risk of metachronous squamous cell carcinoma in the upper aerodigestive tract of Japanese alcoholic men with esophageal squamous cell carcinoma: a long-term endoscopic follow-up study. Cancer Sci 2008;99:1164–71.
7. Hartman M, Czene K, Reilly M, Adolfsson J, Bergh J, Adami HO, Dickman PW, Hall P. Incidence and prognosis of synchronous and metachronous bilateral breast cancer. J Clin Oncol 2007;25:4210–6.
8. Colice GL, Rubins J, Unger M. Follow-up and surveillance of the lung cancer patient following curative-intent therapy. Chest 2003; 123:S272–83.
9. Rex DK, Kahi CJ, Levin B, Smith RA, Bond JH, Brooks D, Burt RW, Byers T, Fletcher RH, Hyman N, Johnson D, Kirk L, et al. Guidelines for colonoscopy surveillance after cancer resection: a consensus update by the American Cancer Society and the US Multi-Society Task Force on Colorectal Cancer. Gastroenterology 2006;130:1865–71.
10. Braakhuis BJ, Tabor MP, Kummer JA, Leemans CR, Brakenhoff RH. A genetic explanation of Slaughter's concept of field cancerization: evidence and clinical implications. Cancer Res 2003;63:1727–30.
11. Maekita T, Nakazawa K, Mihara M, Nakajima T, Yanaoka K, Iguchi M, Arii K, Kaneda A, Tsukamoto T, Tatematsu M, Tamura G, Saito D, et al. High levels of aberrant DNA methylation in *Helicobacter pylori*-infected gastric mucosae and its possible association with gastric cancer risk. Clin Cancer Res 2006;12:989–95.
12. Nakajima T, Maekita T, Oda I, Gotoda T, Yamamoto S, Umemura S, Ichinose M, Sugimura T, Ushijima T, Saito D. Higher methylation levels in gastric mucosae significantly correlate with higher risk of gastric cancers. Cancer Epidemiol Biomarkers Prev 2006;15:2317–21.
13. Kondo Y, Kanai Y, Sakamoto M, Mizokami M, Ueda R, Hirohashi S. Genetic instability and aberrant DNA methylation in chronic hepatitis and cirrhosis—a comprehensive study of loss of heterozygosity and microsatellite instability at 39 loci and DNA hypermethylation on 8 CpG islands in microdissected specimens from patients with hepatocellular carcinoma. Hepatology 2000;32:970–9.
14. Shen L, Kondo Y, Rosner GL, Xiao L, Hernandez NS, Vilaythong J, Houlihan PS, Krouse RS, Prasad AR, Einspahr JG, Buckmeier J, Alberts DS, et al. MGMT promoter methylation and field defect in sporadic colorectal cancer. J Natl Cancer Inst 2005;97:1330–8.
15. Ishii T, Murakami J, Notohara K, Cullings HM, Sasamoto H, Kambara T, Shirakawa Y, Naomoto Y, Ouchida M, Shimizu K, Tanaka N, Jass JR, et al. Oesophageal squamous cell carcinoma may develop within a background of accumulating DNA methylation in normal and dysplastic mucosa. Gut 2007;56:13–19.
16. Yan PS, Venkataramu C, Ibrahim A, Liu JC, Shen RZ, Diaz NM, Centeno B, Weber F, Leu YW, Shapiro CL, Eng C, Yeatman TJ, et al. Mapping geographic zones of cancer risk with epigenetic biomarkers in normal breast tissue. Clin Cancer Res 2006;12:6626–36.
17. Arai E, Kanai Y, Ushijima S, Fujimoto H, Mukai K, Hirohashi S. Regional DNA hypermethylation and DNA methyltransferase (DNMT) 1 protein overexpression in both renal tumors and corresponding nontumorous renal tissues. Int J Cancer 2006;119:288–96.
18. Enomoto S, Maekita T, Tsukamoto T, Nakajima T, Nakazawa K, Tatematsu M, Ichinose M, Ushijima T. Lack of association between CpG island methylator phenotype in human gastric cancers and methylation in their background non-cancerous gastric mucosae. Cancer Sci 2007;98:1853–61.
19. Perri F, Cotugno R, Piepoli A, Merla A, Quitadamo M, Gentile A, Pilotto A, Annese V, Andriulli A. Aberrant DNA methylation in non-neoplastic gastric mucosa of *H. Pylori* infected patients and effect of eradication. Am J Gastroenterol 2007;102:1361–71.
20. Calin GA, Croce CM. MicroRNA signatures in human cancers. Nat Rev Cancer 2006;6:857–66.
21. Esquela-Kerscher A, Slack FJ. Oncomirs—microRNAs with a role in cancer. Nat Rev Cancer 2006;6:259–69.
22. Lujambio A, Ropero S, Ballestar E, Fraga MF, Cerrato C, Setien F, Casado S, Suarez-Gauthier A, Sanchez-Cespedes M, Git A, Spiteri I, Das PP, et al. Genetic unmasking of an epigenetically silenced microRNA in human cancer cells. Cancer Res 2007;67:1424–9.
23. Kozaki K, Imoto I, Mogi S, Omura K, Inazawa J. Exploration of tumor-suppressive microRNAs silenced by DNA hypermethylation in oral cancer. Cancer Res 2008;68:2094–105.
24. Saito Y, Liang G, Egger G, Friedman JM, Chuang JC, Coetzee GA, Jones PA. Specific activation of microRNA-127 with downregulation of the proto-oncogene BCL6 by chromatin-modifying drugs in human cancer cells. Cancer Cell 2006;9:435–43.

25. Moriguchi K, Yamashita S, Tsujino Y, Tatematsu M, Ushijima T. Larger numbers of silenced genes in cancer cell lines with increased de novo methylation of scattered CpG sites. Cancer Lett 2007;249: 178–87.
26. Japanese Gastric Cancer Association. Japanese classification of gastric carcinoma—2nd English edition. Gastric Cancer 1998;1: 10–24.
27. Lauren P. The two histological main types of gastric carcinoma: diffuse and so-called intestinal-type carcinoma. An attempt at a histo-clinical classification. Acta Pathol Microbiol Scand 1965; 64:31–49.
28. Kaneda A, Kaminishi M, Sugimura T, Ushijima T. Decreased expression of the seven ARP2/3 complex genes in human gastric cancers. Cancer Lett 2004;212:203–10.
29. Li B, Carey M, Workman JL. The role of chromatin during transcription. Cell 2007;128:707–19.
30. Lin JC, Jeong S, Liang G, Takai D, Fatemi M, Tsai YC, Egger G, Gal-Yam EN, Jones PA. Role of nucleosomal occupancy in the epigenetic silencing of the MLH1 CpG island. Cancer Cell 2007;12:432–44.
31. Weisenberger DJ, Siegmund KD, Campan M, Young J, Long TI, Faasse MA, Kang GH, Widschwendter M, Weener D, Buchanan D, Koh H, Simms L, et al. CpG island methylator phenotype underlies sporadic microsatellite instability and is tightly associated with BRAF mutation in colorectal cancer. Nat Genet 2006;38:787–93.
32. Ogino S, Odze RD, Kawasaki T, Brahmandam M, Kirkner GJ, Laird PW, Loda M, Fuchs CS. Correlation of pathologic features with CpG island methylator phenotype (CIMP) by quantitative DNA methylation analysis in colorectal carcinoma. Am J Surg Pathol 2006;30: 1175–83.
33. Issa JP, Ahuja N, Toyota M, Bronner MP, Brentnall TA. Accelerated age-related CpG island methylation in ulcerative colitis. Cancer Res 2001;61:3573–7.
34. Ushijima T, Okochi-Takada E. Aberrant methylations in cancer cells: where do they come from? Cancer Sci 2005;96:206–11.
35. Yang N, Coukos G, Zhang L. MicroRNA epigenetic alterations in human cancer: one step forward in diagnosis and treatment. Int J Cancer 2008;122:963–8.
36. Uemura N, Okamoto S, Yamamoto S, Matsumura N, Yamaguchi S, Yamakido M, Taniyama K, Sasaki N, Schlemper RJ. *Helicobacter pylori* infection and the development of gastric cancer. N Engl J Med 2001;345:784–9.
37. Miyazaki T, Murayama Y, Shinomura Y, Yamamoto T, Watabe K, Tsutsui S, Kiyohara T, Tamura S, Hayashi N. E-cadherin gene promoter hypermethylation in *H. pylori*-induced enlarged fold gastritis. Helicobacter 2007;12:523–31.

Carcinogenesis vol.30 no.2 pp.214–221, 2009
doi:10.1093/carcin/bgn268
Advance Access publication November 26, 2008

Genome-wide DNA methylation profiles in both precancerous conditions and clear cell renal cell carcinomas are correlated with malignant potential and patient outcome

Eri Arai, Saori Ushijima, Hiroyuki Fujimoto[1], Fumie Hosoda[2], Tatsuhiro Shibata[2], Tadashi Kondo[3], Sana Yokoi[4], Issei Imoto[4], Johji Inazawa[4], Setsuo Hirohashi and Yae Kanai*

Pathology Division, National Cancer Center Research Institute, 5-1-1 Tsukiji, Chuo-ku, Tokyo 104-0045, Japan, [1]Urology Division, National Cancer Center Hospital, Tokyo 104-0045, Japan, [2]Cancer Genomics Project and [3]Proteome Bioinformatics Project, National Cancer Center Research Institute, Tokyo 104-0045, Japan and [4]Department of Molecular Cytogenetics, Medical Research Institute and School of Biomedical Science, Tokyo Medical and Dental University, Tokyo 113-8510, Japan

*To whom correspondence should be addressed. Tel: +81 3 3542 2511; Fax: +81 3 3248 2463;
Email: ykanai@ncc.go.jp

To clarify genome-wide DNA methylation profiles during multistage renal carcinogenesis, bacterial artificial chromosome array-based methylated CpG island amplification (BAMCA) was performed. Non-cancerous renal cortex tissue obtained from patients with clear cell renal cell carcinomas (RCCs) (N) was at the precancerous stage where DNA hypomethylation and DNA hypermethylation on multiple bacterial artificial chromosome (BAC) clones were observed. By unsupervised hierarchical clustering analysis based on BAMCA data for their N, 51 patients with clear cell RCCs were clustered into two subclasses, Clusters A_N ($n = 46$) and B_N ($n = 5$). Clinicopathologically aggressive clear cell RCCs were accumulated in Cluster B_N, and the overall survival rate of patients in Cluster B_N was significantly lower than that of patients in Cluster A_N. By unsupervised hierarchical clustering analysis based on BAMCA data for their RCCs, 51 patients were clustered into two subclasses, Clusters A_T ($n = 43$) and B_T ($n = 8$). Clinicopathologically aggressive clear cell RCCs were accumulated in Cluster B_T, and the overall survival rate of patients in Cluster B_T was significantly lower than that of patients in Cluster A_T. Multivariate analysis revealed that belonging to Cluster B_T was an independent predictor of recurrence. Cluster B_N was completely included in Cluster B_T, and the majority of the BAC clones that significantly discriminated Cluster B_N from Cluster A_N also discriminated Cluster B_T from Cluster A_T. In individual patients, DNA methylation status in N was basically inherited by the corresponding clear cell RCC. DNA methylation alterations in the precancerous stage may generate more malignant clear cell RCCs and determine patient outcome.

Introduction

It is known that DNA hypomethylation results in chromosomal instability as a result of changes in chromatin structure and that DNA hypermethylation of CpG islands silences tumor-related genes in cooperation with histone modification in human cancers (1–5). Accumulating evidence suggests that alterations of DNA methylation are involved even in the early and the precancerous stages (6,7). On the other hand, in patients with cancers, aberrant DNA methylation is significantly associated with poorer tumor differentiation, tumor aggressiveness and poor prognosis (6,7). Therefore, alterations of DNA methylation may play a significant role in multistage carcinogenesis and can become an indicator for carcinogenetic risk estimation and a biological predictor of poor prognosis in patients with cancers. Recently developed array-based technology for accessing genome-wide DNA methylation status (8–10) is now mainly used to identify tumor-related genes silenced by DNA methylation in human cancers. Subclassification of cancers based on DNA methylation status, which may reflect the distinct epigenetic pathways of carcinogenesis, and DNA methylation profiles, which could become the optimum indicator for carcinogenetic risk estimation and prediction of patient outcome, should be further explored in each organ using array-based approaches.

With respect to renal carcinogenesis, we have reported that accumulation of DNA methylation on C-type CpG islands occurs in a cancer-specific but not age-dependent manner (11), even in non-cancerous renal tissue samples obtained from patients with clear cell renal cell carcinomas (RCCs) (6,7,12). Although precancerous conditions in the kidney have been rarely described, from the viewpoint of altered DNA methylation, non-cancerous renal tissues obtained from patients with clear cell RCCs are considered to already be at the precancerous stage in spite of showing no remarkable histological changes and lacking association with chronic inflammation and persistent infection with viruses or other pathogenic microorganisms. Surprisingly, accumulation of DNA methylation on C-type CpG islands in such non-cancerous renal tissues has been shown to be significantly correlated with higher histological grades of the corresponding clear cell RCCs developing in individual patients (6,7,12). However, since in the previous study we examined DNA methylation status on only a restricted number of CpG islands (12), we were unable to conclude that genome-wide DNA methylation alterations in precancerous conditions generate more malignant RCCs. In the previous study, accumulation of DNA methylation on C-type CpG islands in clear cell RCCs themselves was significantly correlated with tumor aggressiveness and poorer patient outcome (12). However, we were unable to conclude that the examined C-type CpG islands are the optimum prognostic indicator for patients with clear cell RCCs.

In this study, in order to clarify genome-wide DNA methylation profiles during multistage renal carcinogenesis, we performed bacterial artificial chromosome array-based methylated CpG island amplification (BAMCA) (13–15) using a microarray of 4361 bacterial artificial chromosome (BAC) clones (16) in normal renal cortex tissue samples, non-cancerous renal cortex tissue samples obtained from patients with clear cell RCC and the corresponding clear cell RCCs.

Abbreviations: BAC, bacterial artificial chromosome; BAMCA, bacterial artificial chromosome array-based methylated CpG island amplification; RCC, renal cell carcinoma; TNM, tumor–node–metastasis.

Materials and methods

Patients and tissue samples

Paired specimens of cancerous tissue (T1–T51) and corresponding non-cancerous renal cortex tissue showing no remarkable histological changes (N1–N51) were obtained from materials surgically resected from 51 patients (RCC1–RCC 51) with primary clear cell RCC. These patients did not receive preoperative treatment and underwent nephrectomy in 1999–2006 at the National Cancer Center Hospital, Tokyo, Japan. There were 34 men and 17 women with a mean (±SD) age of 59 ± 10 years (range 31–81 years). Histological diagnosis was made in accordance with the World Health Organization classification (17). All the tumors were graded on the basis of

previously described criteria (18) and classified according to the pathological tumor–node–metastasis (TNM) classification (19). The criteria for macroscopic configuration of RCC (12) followed those established for hepatocellular carcinoma: type 3 (contiguous multinodular type) hepatocellular carcinomas show poorer histological differentiation and a higher incidence of intrahepatic metastasis than type 1 (single nodular type) and type 2 (single nodular type with extranodular growth) hepatocellular carcinomas (20). The presence or absence of vascular involvement was examined microscopically on slides stained with hematoxylin–eosin and elastica van Gieson. The presence or absence of tumor thrombi in the main trunk of the renal vein was examined macroscopically. RCC is usually encapsulated by a fibrous capsule and well demarcated and hardly ever contains fibrous stroma between cancer cells (panel T in Figure 1A). Therefore, we were able to obtain cancer cells of high purity from surgical specimens, avoiding contamination with both noncancerous epithelial cells and stromal cells.

For comparison, eight normal renal cortex tissue samples (C1–C8) were obtained from materials surgically resected from eight patients without any primary renal tumor. These patients included five men and three women with a mean (±SD) age of 61 ± 12 years (range 47–81 years). Six of these patients underwent nephroureterectomy for urothelial carcinomas of the ureter, and the other two patients underwent nephrectomy with resection of retroperitoneal sarcoma around the kidney.

High-molecular weight DNA from these fresh frozen tissue samples was extracted using phenol–chloroform, followed by dialysis. Because DNA methylation status is known to be organ specific (21), the reference DNA for analysis of the developmental stages of clear cell RCC should be obtained from the renal cortex and not from other organs or peripheral blood. Therefore, a mixture of normal renal cortex tissue DNA obtained from six male patients (C9–C14) without any primary renal tumor was used as a reference for analyses of male test DNA samples, and a mixture of normal renal cortex tissue DNA obtained from three female patients (C15–C17) without any primary renal tumor was used as a reference for analyses of female test DNA samples.

This study was approved by the Ethics Committee of the National Cancer Center, Tokyo, Japan.

BAMCA

DNA methylation status was analyzed by BAMCA using a custom-made array (MCG Whole Genome Array-4500) harboring 4361 BAC clones throughout chromosomes 1–22 and X and Y (16), as described previously (13–15). Briefly, 5 μg aliquots of test or reference DNA were first digested with 100 U of methylation-sensitive restriction enzyme SmaI and subsequently with 20 U of methylation-insensitive XmaI. Adapters were ligated to XmaI-digested sticky ends, and polymerase chain reaction was performed with an adapter primer set. Test and reference polymerase chain reaction

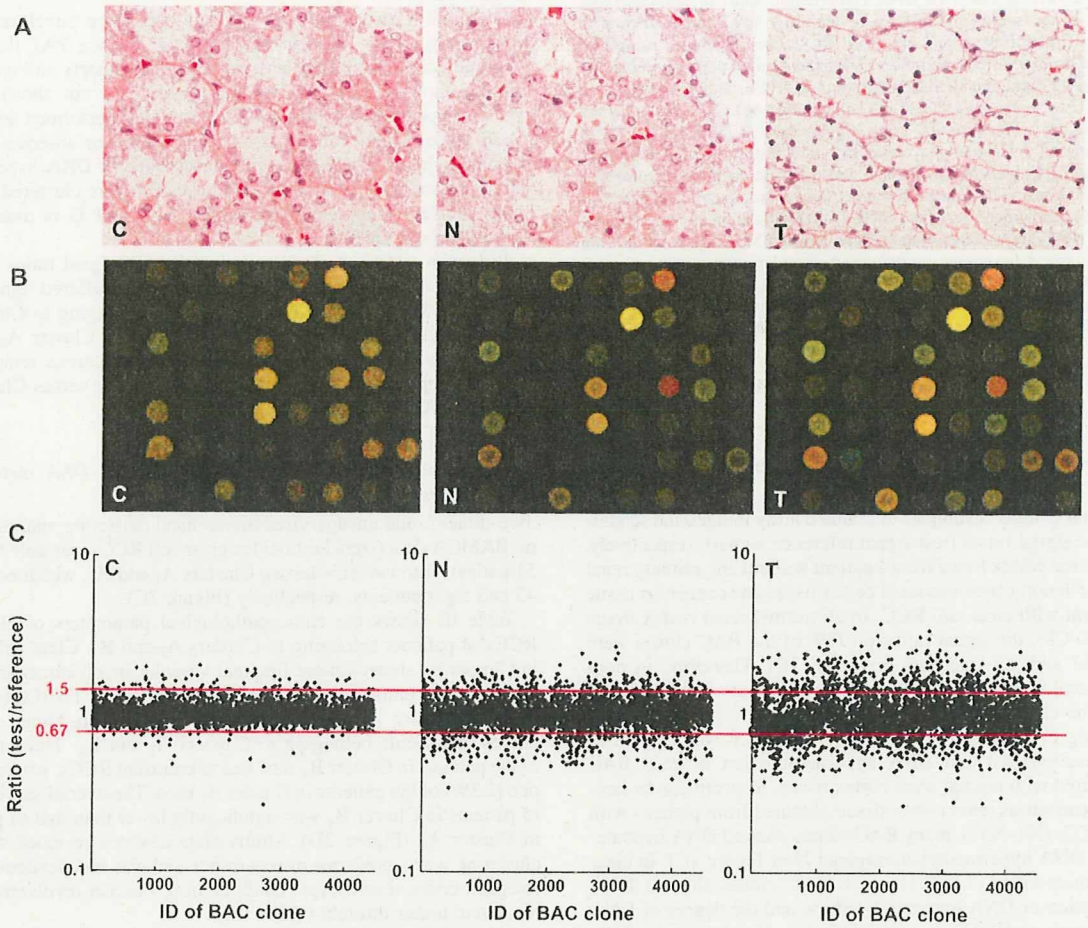

Fig. 1. DNA methylation alterations during multistage renal carcinogenesis. (**A**) Microscopic view of normal renal cortex tissue obtained from a patient without any primary renal tumor (C), non-cancerous renal cortex tissue obtained from a patient with clear cell RCC (N) and clear cell RCC (T). N shows no remarkable histological changes compared with C, i.e. no cytological or structural atypia is evident in N. Since T hardly ever contains fibrous stroma between cancer cells, we were able to obtain cancer cells of high purity, avoiding contamination with stromal cells. Hematoxylin–eosin staining. Original magnification ×20. (**B**) Scanned array images yielded by BAMCA in C, N and T. Test and reference DNA labeled with Cy3 and Cy5 was cohybridized, respectively. (**C**) Scattergrams of the signal ratios (test signal:reference signal) yielded by BAMCA in C, N and T. In all eight C samples (C1–C8), the signal ratios of 97% of BAC clones were between 0.67 and 1.5 (red bars). Therefore, in N and T, DNA methylation status corresponding to a signal ratio of <0.67 and >1.5 was defined as DNA hypomethylation and DNA hypermethylation on each BAC clone compared with C, respectively. Even though N did not show any remarkable histological changes compared with C [panels C and N in (A)], many BAC clones showed DNA hypomethylation or hypermethylation. In T, more BAC clones showed DNA hypomethylation or hypermethylation, and the degree of DNA hypomethylation and hypermethylation, i.e. deviation of the signal ratio from 0.67 or 1.5, was increased in comparison with N.

products were labeled by random priming with Cy3- and Cy5-dCTP (GE Healthcare, Buckinghamshire, UK), respectively, using a BioPrime array CGH genomic labeling system (Invitrogen, Carlsbad, CA) and precipitated together with ethanol in the presence of Cot-I DNA. The mixture was applied to array slides and incubated at 43°C for 72 h. Arrays were scanned with a GenePix Personal 4100A (Axon Instruments, Foster City, CA) and analyzed using GenePix Pro 5.0 imaging software (Axon Instruments) and Acue 2 software (Mitsui Knowledge Industry, Tokyo, Japan). The signal ratios were normalized in each sample to make the mean signal ratios of all BAC clones 1.0.

Statistics

Differences in the average number of BAC clones that showed DNA methylation alterations (DNA hypomethylation and hypermethylation) between non-cancerous renal cortex tissue samples obtained from patients with clear cell RCCs, and the clear cell RCCs themselves, were analyzed using the Mann–Whitney *U*-test. Differences at $P < 0.05$ were considered significant. Two-dimensional unsupervised hierarchical clustering analysis of the patients with clear cell RCCs and the BAC clones based on the signal ratios (test signal: reference signal) obtained by BAMCA in non-cancerous renal cortex tissue samples and those in clear cell RCCs were performed using the Expressionist software program (Gene Data, Basel, Switzerland). Correlations between the subclassification of patients with clear cell RCCs yielded by the unsupervised hierarchical clustering based on DNA methylation status of non-cancerous renal cortex tissue samples (Clusters A_N and B_N) and clinicopathological parameters of the corresponding clear cell RCCs were analyzed using chi-square test. Correlations between the subclassification of patients yielded by the unsupervised hierarchical clustering based on DNA methylation status in clear cell RCCs (Clusters A_T and B_T) and clinicopathological parameters of the RCCs themselves were analyzed using chi-square test. Survival curves of patients belonging to Clusters A_N versus B_N and Clusters A_T versus B_T were calculated by the Kaplan–Meier method, and the differences were compared by the Log-rank test. The Cox proportional hazards multivariate model was used to examine the prognostic impact of the subclassification of patients based on the DNA methylation status of their clear cell RCCs (Clusters A_T and B_T), histological grade, macroscopic configuration, vascular involvement and renal vein tumor thrombi. Differences at $P < 0.05$ were considered significant. BAC clones whose signal ratios were significantly different between Clusters A_N and B_N and Clusters A_T and B_T were each identified by Wilcoxon test ($P < 0.01$).

Results

DNA methylation alterations in samples of both cancerous and non-cancerous renal cortex tissue obtained from patients with clear cell RCCs

Figure 1B and C shows examples of scanned array images and scattergrams of the signal ratios (test signal:reference signal), respectively, for normal renal cortex tissue from a patient without any primary renal tumor and both non-cancerous renal cortex tissue and cancerous tissue from a patient with clear cell RCC. In all normal renal cortex tissue samples (C1–C8), the signal ratios of 97% of the BAC clones were between 0.67 and 1.5 (red bars in Figure 1C). Therefore, in non-cancerous renal cortex tissue obtained from patients with clear cell RCCs and the clear cell RCCs themselves, DNA methylation status corresponding to a signal ratio of <0.67 and >1.5 was defined as DNA hypomethylation and DNA hypermethylation of each BAC clone compared with normal renal cortex tissue, respectively. In samples of non-cancerous renal cortex tissue obtained from patients with clear cell RCCs (N1–N51), many BAC clones showed DNA hypomethylation or DNA hypermethylation (panel N of Figure 1C). In clear cell RCCs themselves (T1–T51), more BAC clones showed DNA hypomethylation or DNA hypermethylation, and the degree of DNA hypomethylation and DNA hypermethylation, i.e. deviation of the signal ratio from 0.67 or 1.5, was increased in comparison with non-cancerous renal cortex tissue samples obtained from patients with clear cell RCCs (panel T of Figure 1C). The average number of BAC clones showing DNA hypomethylation increased significantly from non-cancerous renal cortex tissue samples obtained from patients with clear cell RCCs (93 ± 75) to clear cell RCCs (142 ± 74, $P = 0.0002$). The average number of BAC clones showing DNA hypermethylation also increased significantly in a similar manner (83 ± 73–123 ± 786, $P = 0.004$).

Unsupervised hierarchical clustering of patients with clear cell RCCs based on DNA methylation status of non-cancerous renal cortex tissue samples

By two-dimensional unsupervised hierarchical clustering analysis based on BAMCA data (signal ratios) for non-cancerous renal cortex tissue samples, the 51 patients with clear cell RCCs were clustered into two subclasses, Clusters A_N and B_N, which contained 46 and 5 patients, respectively (Figure 2A).

Table IA shows the clinicopathological parameters of clear cell RCCs of patients belonging to Clusters A_N and B_N. The corresponding clear cell RCCs of patients in Cluster B_N showed more frequent macroscopically evident multinodular (type 3) growth, vascular involvement and renal vein tumor thrombi and showed higher pathological TNM stages than those in Cluster A_N. Figure 2B shows the Kaplan–Meier survival curves of patients belonging to Clusters A_N and B_N. The period covered ranged from 88 to 2801 days (mean, 1679 days). Three (60%) of the patients in Cluster B_N died of recurrent RCC, whereas only one (2%) of the patients in Cluster A_N died. The overall survival rate of patients in Cluster B_N was significantly lower than that of patients in Cluster A_N (Figure 2B).

Although Cluster A_N was divided into three subclusters, A_{N1} ($n = 3$), A_{N2} ($n = 19$) and A_{N3} ($n = 24$) (Figure 2A), there were no significant correlations between these subclusters and any of the clinicopathological parameters examined (data not shown). Even when unsupervised hierarchical clustering was performed separately, based not on signal ratios but on the presence or absence of DNA hypomethylation and the presence or absence of DNA hypermethylation, the majority of patients in Cluster B_N were clustered into the same subclass (supplementary Figure S1A and B is available at *Carcinogenesis* Online).

Wilcoxon test ($P < 0.01$) revealed that the signal ratios of 1143 BAC clones in non-cancerous renal cortex tissue differed significantly between Clusters A_N and B_N: e.g. patients belonging to Cluster B_N were completely discriminated from patients in Cluster A_N by the DNA methylation status of samples of non-cancerous renal cortex tissue for representative BAC clones (Cluster A_N versus Cluster B_N in Figure 3A) out of the 1143 BAC clones.

Unsupervised hierarchical clustering based on DNA methylation status of clear cell RCCs

Two-dimensional unsupervised hierarchical clustering analysis based on BAMCA data (signal ratios) for clear cell RCCs was able to group 51 patients into two subclasses, Clusters A_T and B_T, which contained 43 and eight patients, respectively (Figure 2C).

Table IB shows the clinicopathological parameters of clear cell RCCs of patients belonging to Clusters A_T and B_T. Clear cell RCCs in Cluster B_T showed more frequent vascular involvement and renal vein tumor thrombi and showed higher pathological TNM stages than those in Cluster A_T. Figure 2D shows the Kaplan–Meier survival curves of patients belonging to Clusters A_T and B_T. Three (37.5%) of the patients in Cluster B_T died due to recurrent RCCs, whereas only one (2.3%) of the patients in Cluster A_T died. The overall survival rate of patients in Cluster B_T was significantly lower than that of patients in Cluster A_T (Figure 2D). Multivariate analysis revealed that our clustering was a predictor of recurrence and was independent of histological grade, macroscopic configuration, vascular involvement and renal vein tumor thrombi (Table II).

Although Cluster A_T was divided into four subclusters, A_{T1} ($n = 8$), A_{T2} ($n = 12$), A_{T3} ($n = 13$) and A_{T4} ($n = 10$) (Figure 2B), there were no significant correlations between these subclusters and any of the clinicopathological parameters examined (data not shown). Even when unsupervised hierarchical clustering was performed separately, based not on signal ratios but on the presence or absence of DNA hypomethylation and the presence or absence of DNA hypermethylation, the majority of patients in Cluster B_T were clustered into the same subclass (supplementary Figure S1C and D is available at *Carcinogenesis* Online).

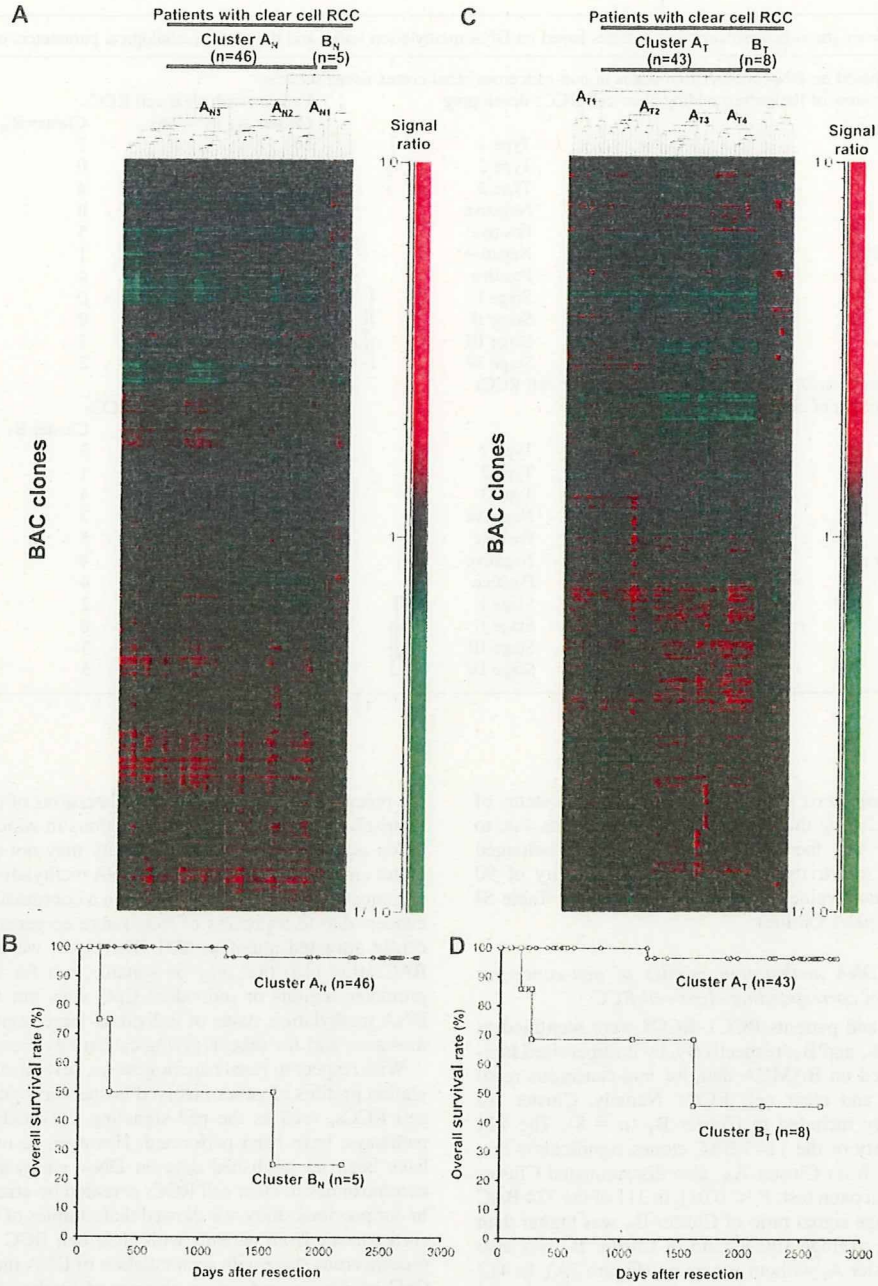

Fig. 2. Two-dimensional unsupervised hierarchical clustering analysis based on BAMCA data (signal ratios) in non-cancerous renal cortex tissue samples showing no remarkable histological changes (A) and clear cell RCCs (C) and Kaplan–Meier survival curves of patients with clear cell RCCs (B and D). (**A**) Fifty-one patients with clear cell RCC were hierarchically clustered into two subclasses, Clusters A_N ($n = 46$) and B_N ($n = 5$), based on DNA methylation status of their non-cancerous renal cortex tissue samples. DNA hypomethylation, normomethylation (DNA methylation status corresponding to a signal ratio of between 0.67 and 1.5) and hypermethylation on each BAC clone are shown in green, black and red, respectively. The signal ratio is shown in the color range maps. The cluster trees for patients and BAC clones are shown at the top and left of the panel, respectively. (**B**) The overall survival rate of patients in Cluster B_N (square) defined on the basis of DNA methylation status in their non-cancerous renal cortex tissue samples was significantly lower than that of patients in Cluster A_N (circle) ($P = 0.0000000613$, Log-rank test). (**C**) Fifty-one patients were hierarchically clustered into two subclasses, Clusters A_T ($n = 43$) and B_T ($n = 8$), based on the DNA methylation status of their clear cell RCCs. (**D**) The overall survival rate of patients in Cluster B_T (square) defined on the basis of DNA methylation status in their clear cell RCCs was significantly lower than that of patients in Cluster A_T (circle) ($P = 0.0000413$, Log-rank test).

Wilcoxon test ($P < 0.01$) revealed that the signal ratios of 1111 BAC clones in clear cell RCCs were differed significantly between Clusters A_T and B_T. In particular, patients belonging to Cluster B_T were completely discriminated from patients belonging to Cluster A_T based on the DNA methylation status of 14 BAC clones (Cluster A_T versus Cluster B_T in Figure 3A). In other words, DNA methylation status of the 14 BAC clones was able to determine whether or not patients in this cohort belonged to Cluster B_T, a significant prognostic indicator, with a sensitivity and specificity of 100% using the cutoff values shown in Figure 3A and supplementary Table

Table I. Correlation between the subclassification of patients based on DNA methylation status and the clinicopathological parameters of clear cell RCCs

(A) Clusters A_N and B_N based on DNA methylation status in non-cancerous renal cortex tissue samples			
Clinicopathological parameters of the corresponding clear cell RCCs developing in individual patients		Patients with clear cell RCCs		P^a
		Cluster A_N (n = 46)	Cluster B_N (n = 5)	
Macroscopic finding	Type 1	26	1	0.0248
	Type 2	10	0	
	Type 3	10	4	
Vascular involvement	Negative	38	0	0.0005
	Positive	8	5	
Renal vein tumor thrombi	Negative	41	1	0.0017
	Positive	5	4	
Pathological TNM stage	Stage I	29	0	0.0195
	Stage II	1	0	
	Stage III	13	3	
	Stage IV	3	2	
(B) Clusters A_T and B_T based on DNA methylation status in clear cell RCCs				
Clinicopathalogical parameters of clear cell RCCs		Patients with clear cell RCCs		P^a
		Cluster A_T (n = 43)	Cluster B_T (n = 8)	
Macroscopic finding	Type 1	24	3	NS[b]
	Type 2	9	1	
	Type 3	10	4	
Vascular involvement	Negative	35	3	0.0297
	Positive	8	5	
Renal vein tumor thrombi	Negative	38	4	0.0349
	Positive	5	4	
Pathological TNM stage	Stage I	27	2	0.0263
	Stage II	1	0	
	Stage III	13	3	
	Stage IV	2	3	

[a]Chi-square test.
[b]Not significant.

SI (available at *Carcinogenesis* Online). DNA methylation status of the 70 BAC clones, including the above 14 BAC clones, was able to determine whether or not the patients in this cohort belonged to Cluster B_T, with a sensitivity of 100% and a specificity of 90 or >90%, using the cutoff values shown in supplementary Table SI (available at *Carcinogenesis* Online).

Comparison between DNA methylation profiles of non-cancerous renal tissue and those of corresponding clear cell RCC

Patients RCC1–RCC5 and patients RCC1–RCC8 were identified as belonging to Clusters B_N and B_T, respectively, by unsupervised hierarchical clustering based on BAMCA data for non-cancerous renal cortex tissue samples and clear cell RCCs. Namely, Cluster B_N (n = 5) was completely included in Cluster B_T (n = 8). The 724 BAC clones, the majority of the 1143 BAC clones significantly discriminating Cluster B_N from Cluster A_N, also discriminated Cluster B_T from Cluster A_T (Wilcoxon test, $P < 0.01$). In 311 of the 724 BAC clones, where the average signal ratio of Cluster B_N was higher than that of Cluster A_N, the average signal ratio of Cluster B_T was also higher than that of Cluster A_T without exception (Figure 3A). In 413 of the 724 BAC clones, where the average signal ratio of Cluster B_N was lower than that of Cluster A_N, the average signal ratio of Cluster B_T was also lower than that of Cluster A_T without exception (Figure 3A). Figure 3B shows the signal ratios of non-cancerous renal cortex tissue samples and clear cell RCCs for all 51 patients for a representative BAC clone (RP11-44F3). In individual patients, DNA methylation status in the non-cancerous renal cortex tissue was basically inherited by the corresponding clear cell RCC (Figure 3B).

Discussion

Many researchers in this field use arrays in which the promoter regions are enriched as probes to identify the genes methylated in cancer cells (8–10). However, the promoter regions of specific genes are not the only target of DNA methylation alterations in human cancers. DNA methylation status in genomic regions not directly participating in gene silencing, such as the edges of CpG islands, may be altered at the precancerous stage before the alterations of the promoter regions themselves occur (22). Genomic regions in which DNA hypomethylation affects chromosomal instability may not be contained in promoter arrays. Moreover, aberrant DNA methylation of large regions of chromosomes, which are regulated in a coordinated manner in human cancers due to a process of long-range epigenetic silencing, has recently attracted attention (23). Therefore, we used a custom-made BAC array (16) that may be suitable, not for focusing on specific promoter regions or individual CpG sites but for overviewing the DNA methylation status of individual large regions among all chromosomes and for subclassifying cancers by hierarchical clustering.

With respect to renal carcinogenesis, several studies of DNA methylation profiles of genes involved in specific signal pathways in clear cell RCCs, such as the p53-signaling (24) and Wnt-signaling (25) pathways, have been performed. However, to our knowledge, there have been no published data on DNA methylation profiles for all chromosomes in clear cell RCCs revealed by array-based technology. In our previous study, we showed that samples of non-cancerous renal cortex tissue from patients with clear cell RCC were already at the precancerous stage with accumulation of DNA methylation on C-type CpG islands, in spite of an absence of marked histological changes (6,7,12). In the present study, genome-wide DNA methylation alterations (both hypomethylation and hypermethylation) in samples of non-cancerous renal cortex tissue from patients with clear cell RCC were confirmed by BAMCA (panel N of Figure 1B and C). We then performed unsupervised hierarchical clustering analysis based on the genome-wide DNA methylation status of the non-cancerous renal cortex tissue samples, and as a result, 51 patients were subclassified into Clusters A_N and B_N. Corresponding clear cell RCCs showing multinodular growth, vascular involvement, renal vein tumor thrombi and higher pathological TNM stages were found to be accumulated in Cluster B_N. Although subclassification of precancerous tissue by unsupervised hierarchical clustering analysis on the basis of genome-wide DNA methylation profiles has never been performed for specific organs, our Clusters A_N and B_N can be considered clinicopathologically valid.

The significant correlation between genome-wide DNA methylation profiles of samples of non-cancerous renal cortex tissue and

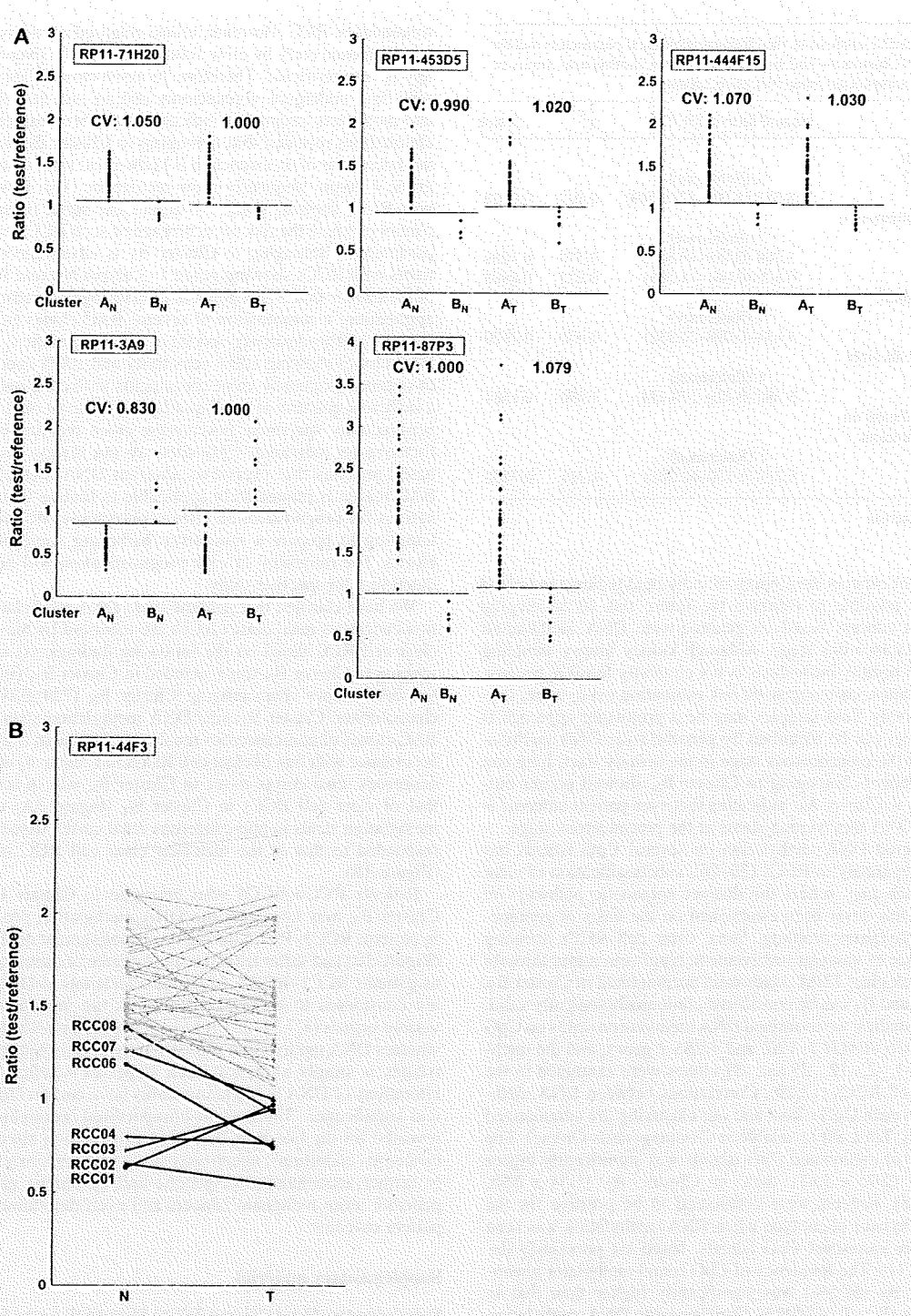

Fig. 3. (**A**) Scattergrams of the signal ratios in non-cancerous renal cortex tissue samples (Cluster A_N versus Cluster B_N) and in clear cell RCCs (Cluster A_T versus Cluster B_T) on representative BAC clones, RP11-71H20, RP11-453D5, RP11-444F15, RP11-3A9 and RP11-87P3. Using the cutoff values (CVs) described in each panel, patients belonging to Cluster B_N were completely discriminated from patients in Cluster A_N based on the DNA methylation status of non-cancerous renal cortex tissue samples. Using the cutoff value described in each panel, patients belonging to Cluster B_T were completely discriminated from patients in Cluster A_T based on the DNA methylation status of the clear cell RCCs. When the signal ratios of Cluster B_N were lower than those of Cluster A_N, the signal ratios of Cluster B_T were also lower than those of Cluster A_T (RP11-71H20, RP11-453D5, RP11-444F15 and RP11-87P3). When the signal ratios of Cluster B_N were higher than those of Cluster A_N, the signal ratios of Cluster B_T were also higher than those in Cluster A_T (RP11-3A9). (**B**) The signal ratios of non-cancerous renal cortex tissue (N) and clear cell RCC (T) for all 51 patients on a representative BAC clone (RP11-44F3). DNA methylation status in N was basically inherited in the corresponding T developing in the individual patient. Gray bar, patients belonging to Cluster A_T; black bar, patients belonging to Cluster B_T. The case numbers of patients belonging to Cluster B_T (RCC1–RCC8) are also shown on the left side. Patients RCC6–RCC8 did not belong to Cluster B_N, but later gained the same DNA methylation profiles as those of patients RCC1–RCC5 during the development of T from N, and joined Cluster B_T.

Table II. Multivariate analysis of the clinicopathological parameters and the subclassification (Clusters A_T and B_T) based on DNA methylation status of cancerous tissue samples as predictors of recurrence

Parameters	Hazard ratio (95% CI)	χ^2	*P* value
Histological grade			
Grade 1, 2 or 3	1 (Reference)		
Grade 4	118.582 (5.186–2711.249)	8.947	0.0028
Macroscopic configuration			
Type 1	1 (Reference)		
Type 2	5.309 (0.689–40.887)	2.570	0.1089
Type 3	0.820 (0.061–11.005)	0.022	0.8808
Vascular involvement			
Negative	1 (Reference)		
Positive	1.434 (0.098–20.932)	0.070	0.7920
Renal vein tumor thrombi			
Negative	1 (Reference)		
Positive	8.780 (0.429–179.734)	1.990	0.1584
Subclassification based on DNA methylation status			
Cluster A_T	1 (Reference)		
Cluster B_T	8.317 (1.100–62.901)	4.211	0.0402

CI, confidence interval.

aggressiveness of cancers developing in individual patients indicated that it may be possible to estimate the future risk of developing more malignant cancers based on genome-wide DNA methylation status at the precancerous stage. Although kidney biopsy sampling for screening of healthy individuals is not clinically feasible because of its invasive nature, carcinogenetic risk estimation using urine, sputum and other body fluid samples may be a promising approach if optimal indicators can be identified by genome-wide DNA methylation profiling at the precancerous stage in the urinary tract, lung and other organs. Patients belonging to Cluster B_N showed poorer outcome than those in Cluster A_N, indicating that even patient outcome is determined by DNA methylation status at the precancerous stage.

Although altered DNA methylation on several CpG islands has been reported separately in RCCs (26–28), subclassification of clear cell RCCs, which may reflect the distinct epigenetic pathways of carcinogenesis, has never been established on the basis of genome-wide DNA methylation profiling. Since clear cell RCCs showing a higher incidence of vascular involvement, renal vein tumor thrombi and higher pathological TNM stages were accumulated in Cluster B_T, our Clusters A_T and B_T can be considered clinicopathologically valid. In our previous studies, we examined DNA methylation status on CpG islands for the *p16*, *hMLH 1*, *VHL* and *THBS 1* genes, and the methylated in tumor-1, -2, -12, -25 and -31 clones were examined in the same 51 clear cell RCCs (12,29). Correlations between DNA methylation status on each CpG island and our clustering are summarized in supplementary Table SII (available at *Carcinogenesis* Online). The average number of methylated CpG islands was significantly higher in Cluster B_T (2.75 ± 1.67) than in Cluster A_T (1.54 ± 0.98, $P = 0.01867318$). Patients were considered to be positive for the CpG island methylator phenotype when DNA methylation was seen on three or more examined CpG islands, based on previously described criteria (11). The frequency of CpG island methylator phenotype in Cluster B_T (62.5%) was significantly higher than that in Cluster A_T (16%, $P = 0.0174969$). Genome-wide DNA methylation alterations consisting of both hypomethylation and hypermethylation of DNA revealed by BAMCA in Cluster B_T are associated with regional DNA hypermethylation on CpG islands and participate in malignant progression of clear cell RCCs. Moreover, patients belonging to Cluster B_T showed poorer outcome than those in Cluster A_T, indicating that prognostication of clear cell RCCs using DNA methylation status as an indicator is a promising approach.

Some RCCs relapse and metastasize to distant organs, even if resection has been considered complete (17,30). Recently, immunotherapy (31) and novel targeting agents (32) have been developed for treatment of RCC. However, unless relapsed or metastasized tumors are diagnosed early by close follow-up, the effectiveness of any therapy is very restricted. Therefore, to assist close follow-up of patients who have undergone nephrectomy and are still at risk of recurrence and metastasis, prognostic indicators have been explored. Multivariate analysis revealed that belonging to Cluster B_T was an independent predictor of recurrence. It is known that sarcomatoid RCCs with grade 4 atypia frequently show recurrence (18). However, patients with RCCs showing grade 1–3 atypia also suffer recurrence, and we cannot estimate the risk of recurrence of such RCCs based on known parameters. Belonging to Cluster B_T is advantageous even to patients with RCCs showing grade 1–3 atypia because it is a predictor of recurrence that is independent of histological grading. For clinical application, a combination of several BAC clones from the 70 that showed 100% sensitivity and 90 or >90% specificity (including 14 BAC clones showing 100% sensitivity and 100% specificity) can be of optimal prognostic value for patients with clear cell RCCs. Since a sufficient quantity of good-quality DNA can be obtained from each nephrectomy specimen, polymerase chain reaction-based analyses focusing on individual CpG sites are not always required. Array-based analysis that overviews aberrant DNA methylation of each BAC region is immediately applicable to routine laboratory examinations for prognostication after nephrectomy. We are currently attempting to prepare a mini-array harboring some of the 70 BAC clones. The reliability of such prognostication will need to be validated in a prospective study.

We have clarified that genome-wide DNA methylation profiles of non-cancerous renal cortex tissue are inherited by the corresponding clear cell RCC based on the following findings: (i) all patients belonging to Cluster B_N were included in Cluster B_T; (ii) a majority of the BAC clones characterizing Cluster B_N (724 BAC clones) also characterized Cluster B_T; (iii) DNA methylation status on such 724 BAC clones of non-cancerous renal cortex tissue in Cluster A_N was in accordance with that of clear cell RCCs in Cluster A_T and that of non-cancerous renal cortex tissue in Cluster B_N was in accordance with that of clear cell RCCs in Cluster B_T (Figure 3A) and (iv) DNA methylation status in non-cancerous renal cortex tissue basically corresponded to that in the matching clear cell RCC in each patient (Figure 3B).

Patients RCC6–RCC8 who belonged to Cluster B_T but not to Cluster B_N may later gain the DNA methylation profiles observed in patients RCC1–RCC5 during the establishment of clear cell RCCs (Figure 3B) and suffer from the same degree of tumor aggressiveness as patients RCC1–RCC5. Although alterations of DNA methylation are considered to be involved even in the precancerous stage in various organs (6,7,33–35), it has not yet been clarified for any organ whether DNA methylation status on only a restricted number of CpG islands is simply altered at such stages or whether genome-wide alterations of DNA methylation status have certain clinicopathological significance. The present unsupervised hierarchical clustering revealed for the first time that DNA methylation alterations in precancerous conditions, which may not occur randomly but are prone to further accumulation of genetic and epigenetic alterations, can generate more malignant cancers and even determine the ultimate patient outcome.

Supplementary material

Supplementary Figure S1 and Tables SI and SII can be found at http://carcin.oxfordjournals.org/

Funding

Grant-in-Aid for the Third Term Comprehensive 10-Year Strategy for Cancer Control from the Ministry of Health, Labor and Welfare of Japan; Grant-in-Aid for Cancer Research from the Ministry of Health, Labor and Welfare of Japan; New Energy and Industrial Technology Development Organization; Program for Promotion of Fundamental Studies in Health Sciences of the National Institute of Biomedical

Innovation. Funding to pay the Open Access publication charges for this article was provided by a Grant-in-Aid for the Third Term Comprehensive 10-Year Strategy for Cancer Control from the Ministry of Health, Labor and Welfare of Japan.

Acknowledgements

Conflict of Interest Statement: None declared.

References

1. Jones,P.A. *et al.* (2002) The fundamental role of epigenetic events in cancer. *Nat. Rev. Genet.*, **3**, 415–428.
2. Eden,A. *et al.* (2003) Chromosomal instability and tumors promoted by DNA hypomethylation. *Science*, **300**, 455.
3. Baylin,S.B. *et al.* (2006) Epigenetic gene silencing in cancer—a mechanism for early oncogenic pathway addiction? *Nat. Rev. Cancer*, **6**, 107–116.
4. Gronbaek,K. *et al.* (2007) Epigenetic changes in cancer. *APMIS*, **115**, 1039–1159.
5. Feinberg,A.P. (2007) Phenotypic plasticity and the epigenetics of human disease. *Nature*, **447**, 433–440.
6. Kanai,Y. *et al.* (2007) Alterations of DNA methylation associated with abnormalities of DNA methyltransferases in human cancers during transition from a precancerous to a malignant state. *Carcinogenesis*, **28**, 2434–2442.
7. Kanai,Y. (2008) Alterations of DNA methylation and clinicopathological diversity of human cancers. *Pathol. Int.*, **58**, 544–558.
8. Estecio,M.R. *et al.* (2007) High-throughput methylation profiling by MCA coupled to CpG island microarray. *Genome Res.*, **17**, 1529–1536.
9. Jacinto,F.V. *et al.* (2007) Discovery of epigenetically silenced genes by methylated DNA immunoprecipitation in colon cancer cells. *Cancer Res.*, **67**, 11481–11486.
10. Nielander,I. *et al.* (2007) Combining array-based approaches for the identification of candidate tumor suppressor loci in mature lymphoid neoplasms. *APMIS*, **115**, 1107–1134.
11. Toyota,M. *et al.* (1999) CpG island methylator phenotype in colorectal cancer. *Proc. Natl Acad. Sci. USA*, **96**, 8681–8686.
12. Arai,E. *et al.* (2006) Regional DNA hypermethylation and DNA methyltransferase (DNMT) 1 protein overexpression in both renal tumors and corresponding nontumorous renal tissues. *Int. J. Cancer*, **119**, 288–296.
13. Misawa,A. *et al.* (2005) Methylation-associated silencing of the nuclear receptor 1I2 gene in advanced-type neuroblastomas, identified by bacterial artificial chromosome array-based methylated CpG island amplification. *Cancer Res.*, **65**, 10233–10242.
14. Sugino,Y. *et al.* (2007) Epigenetic silencing of prostaglandin E receptor 2 (PTGER2) is associated with progression of neuroblastomas. *Oncogene*, **26**, 7401–7413.
15. Tanaka,K. *et al.* (2007) Frequent methylation-associated silencing of a candidate tumor-suppressor, CRABP1, in esophageal squamous-cell carcinoma. *Oncogene*, **26**, 6456–6468.
16. Inazawa,J. *et al.* (2004) Comparative genomic hybridization (CGH)-arrays pave the way for identification of novel cancer-related genes. *Cancer Sci.*, **95**, 559–563.
17. Eble,J.N. *et al.* (2004) *Renal Cell Carcinoma. World Health Organization Classification of Tumours. Pathology and Genetics. Tumours of the Urinary System and Male Genital Organs*, IARC Press, Lyon, 10–43.
18. Fuhrman,S.A. *et al.* (1982) Prognostic significance of morphologic parameters in renal cell carcinoma. *Am. J. Surg. Pathol.*, **6**, 655–663.
19. Sobin,L.H. *et al.* (2002) *International Union Against Cancer (UICC). TNM Classification of Malignant Tumors*, 6th edn. Wiley-Liss, New York, NY, 193–195.
20. Kanai,T. *et al.* (1987) Pathology of small hepatocellular carcinoma. A proposal for a new gross classification. *Cancer*, **60**, 810–819.
21. Illingworth,R. *et al.* (2008) A novel CpG island set identifies tissue-specific methylation at developmental gene loci. *PLoS Biol.*, **6**, e22.
22. Maekita,T. *et al.* (2006) High levels of aberrant DNA methylation in *Helicobacter pylori*-infected gastric mucosae and its possible association with gastric cancer risk. *Clin. Cancer Res.*, **12**, 989–995.
23. Frigola,J. *et al.* (2006) Epigenetic remodeling in colorectal cancer results in coordinate gene suppression across an entire chromosome band. *Nat. Genet.*, **38**, 540–549.
24. Christoph,F. *et al.* (2006) Promoter hypermethylation profile of kidney cancer with new proapoptotic p53 target genes and clinical implications. *Clin. Cancer Res.*, **12**, 5040–5046.
25. Urakami,S. *et al.* (2006) Wnt antagonist family genes as biomarkers for diagnosis, staging, and prognosis of renal cell carcinoma using tumor and serum DNA. *Clin. Cancer Res.*, **12**, 6989–6997.
26. Ibanez de Caceres,I. *et al.* (2006) Identification of novel target genes by an epigenetic reactivation screen of renal cancer. *Cancer Res.*, **66**, 5021–5028.
27. Costa,V.L. *et al.* (2007) Quantitative promoter methylation analysis of multiple cancer-related genes in renal cell tumors. *BMC Cancer*, **7**, 133.
28. Morris,M.R. *et al.* (2008) Functional epigenomics approach to identify methylated candidate tumour suppressor genes in renal cell carcinoma. *Br. J. Cancer*, **98**, 496–501.
29. Arai,E. *et al.* (2008) Genetic clustering of clear cell renal cell carcinoma based on array-CGH: its association with DNA methylation alteration and patient outcome. *Clin. Cancer Res.*, **14**, 5531–5539.
30. Jones,J. *et al.* (2007) Genomics of renal cell cancer: the biology behind and the therapy ahead. *Clin. Cancer Res.*, **13**, 685s–692s.
31. Guida,M. *et al.* (2007) Immunotherapy for metastatic renal cell carcinoma: is it a therapeutic option yet? *Ann. Oncol.*, **18** (suppl. 6), vi149–52.
32. Patel,P.H. *et al.* (2006) Targeting von Hippel-Lindau pathway in renal cell carcinoma. *Clin. Cancer Res.*, **12**, 7215–7520.
33. Kanai,Y. *et al.* (1996) Aberrant DNA methylation on chromosome 16 is an early event in hepatocarcinogenesis. *Jpn. J. Cancer Res.*, **87**, 1210–1217.
34. Eguchi,K. *et al.* (1997) DNA hypermethylation at the D17S5 locus in non-small cell lung cancers: its association with smoking history. *Cancer Res.*, **57**, 4913–4915.
35. Peng,D.F. *et al.* (2006) DNA methylation of multiple tumor-related genes in association with overexpression of DNA methyltransferase 1 (DNMT1) during multistage carcinogenesis of the pancreas. *Carcinogenesis*, **27**, 1160–1168.

Received September 1, 2008; revised November 12, 2008; accepted November 20, 2008

Int. J. Cancer: **125,** 2854–2862 (2009)

Genome-wide DNA methylation profiles in liver tissue at the precancerous stage and in hepatocellular carcinoma

Eri Arai[1], Saori Ushijima[1], Masahiro Gotoh[1], Hidenori Ojima[1], Tomoo Kosuge[2], Fumie Hosoda[3], Tatsuhiro Shibata[3], Tadashi Kondo[4], Sana Yokoi[5], Issei Imoto[5], Johji Inazawa[5], Setsuo Hirohashi[1] and Yae Kanai[1]*

[1]*Pathology Division, National Cancer Center Research Institute, Tokyo, Japan*
[2]*Hepatobiliary and Pancreatic Surgery Division, National Cancer Center Hospital, Tokyo, Japan*
[3]*Cancer Genomics Project, National Cancer Center Research Institute, Tokyo, Japan*
[4]*Proteome Bioinformatics Project, National Cancer Center Research Institute, Tokyo, Japan*
[5]*Department of Molecular Cytogenetics, Medical Research Institute and School of Biomedical Science, Tokyo Medical and Dental University, Tokyo, Japan*

To clarify genome-wide DNA methylation profiles during hepatocarcinogenesis, bacterial artificial chromosome (BAC) array-based methylated CpG island amplification was performed on 126 tissue samples. The average numbers of BAC clones showing DNA hypo- or hypermethylation increased from noncancerous liver tissue obtained from patients with hepatocellular carcinomas (HCCs) (N) to HCCs. N appeared to be at the precancerous stage, showing DNA methylation alterations that were correlated with the future development of HCC. Using Wilcoxon test, 25 BAC clones, whose DNA methylation status was inherited by HCCs from N and were able to discriminate 15 N samples from 10 samples of normal liver tissue obtained from patients without HCCs (C) with 100% sensitivity and specificity, were identified. The criteria using the 25 BAC clones were able to discriminate 24 additional N samples from 26 C samples in the validation set with 95.8% sensitivity and 96.2% specificity. Using Wilcoxon test, 41 BAC clones, whose DNA methylation status was able to discriminate patients who survived more than 4 years after hepatectomy from patients who suffered recurrence within 6 months and died within a year after hepatectomy, were identified. The DNA methylation status of the 41 BAC clones was correlated with the cancer-free and overall survival rates of patients with HCC. Multivariate analysis revealed that satisfying the criteria using the 41 BAC clones was an independent predictor of overall outcome. Genome-wide alterations of DNA methylation may participate in hepatocarcinogenesis from the precancerous stage, and DNA methylation profiling may provide optimal indicators for carcinogenetic risk estimation and prognostication.

Key words: bacterial artificial chromosome array-based methylated CpG island amplification; hepatocellular carcinoma; multistage carcinogenesis; precancerous condition; prognostication

Alteration of DNA methylation is one of the most consistent epigenetic changes in human cancers.[1,2] It is known that DNA hypomethylation results in chromosomal instability as a result of changes in the chromatin structure, and that DNA hypermethylation of CpG islands silences tumor-related genes in cooperation with histone modification in human cancers.[3,4]

With respect to hepatocarcinogenesis, we have shown that alterations of DNA methylation at multiple chromosomal loci can be detected even in noncancerous liver tissue showing chronic hepatitis or cirrhosis, which are widely considered to be precancerous conditions, but not in normal liver tissue, using classical Southern blotting analysis.[5] This was one of the earliest reports of alterations of DNA methylation at the precancerous stage. Multiple tumor-related genes, such as the *E-cadherin*[6,7] and *hypermethylated-in-cancer (HIC)-1*[8] genes, are silenced by DNA hypermethylation in hepatocellular carcinomas (HCCs). DNA methyltransferase (DNMT) 1 expression is significantly higher even in noncancerous liver tissue showing chronic hepatitis or cirrhosis than in the normal liver tissue and is even higher in HCCs.[9,10] DNMT1 overexpression is also correlated with poorer tumor differentiation, portal vein involvement and intrahepatic metastasis of HCCs and poorer patient outcome.[11] On the other hand, overexpression of DNMT3b4, an inactive splice variant of DNMT3b, may lead to chromosomal instability through induction of DNA hypomethylation in pericentromeric satellite regions during hepatocarcinogenesis.[12]

Because aberrant DNA methylation is one of the earliest molecular events during hepatocarcinogenesis and also participates in malignant progression,[13,14] it may be possible to estimate the future risk of developing more malignant HCCs on the basis of DNA methylation status. However, only a few previous studies focusing on HCCs have used recently developed array-based technology for assessing genome-wide DNA methylation status,[15] and such studies have focused mainly on identification of tumor-related genes that are silenced by DNA methylation. DNA methylation profiles, which could become the optimum indicator for carcinogenetic risk estimation and prediction of patient outcome, should therefore be further explored during hepatocarcinogenesis using array-based approaches.

In this study, to clarify genome-wide DNA methylation profiles during multistage hepatocarcinogenesis, we performed bacterial artificial chromosome (BAC) array-based methylated CpG island amplification (BAMCA)[16–18] using a microarray of 4,361 BAC clones[19] in the normal liver tissue obtained from patients without HCCs, noncancerous liver tissue obtained from patients with HCCs, and in HCCs themselves.

Material and methods

Patients and tissue samples

As a learning cohort, 15 samples of the noncancerous liver tissue (N1 to N15) and 19 primary HCCs (T1 to T19) were obtained from surgically resected specimens from 16 patients who underwent partial hepatectomy at the National Cancer Center Hospital, Tokyo, Japan. The patients comprised 13 men and 3 women with a mean (±SD) age of 64.9 ± 7.4 years. Of these, 7 were positive for hepatitis B virus (HBV) surface antigen (HBs-Ag), 8 were positive for anti-hepatitis C virus (HCV) antibody (anti-HCV) and 1 was negative for both. Histological examination of the noncancerous liver tissue samples revealed findings compatible with chronic hepatitis in 5 and cirrhosis in 9 and no remarkable histological findings in 1.

Additional Supporting Information may be found in the online version of this article.

Grant sponsors: Ministry of Health, Labor and Welfare of Japan (Third Term Comprehensive 10-Year Strategy for Cancer Control and Cancer Research), New Energy and Industrial Technology Development Organization (NEDO), National Institute of Biomedical Innovation (NiBio) (Program for Promotion of Fundamental Studies in Health Sciences).

***Correspondence to:** Pathology Division, National Cancer Center Research Institute, 5-1-1 Tsukiji, Chuo-ku, Tokyo 104-0045, Japan. Fax: +81-3-3248-2463. E-mail: ykanai@ncc.go.jp

Received 3 February 2009; Accepted after revision 25 June 2009
DOI 10.1002/ijc.24708
Published online 30 June 2009 in Wiley InterScience (www.interscience.wiley.com).

For the comparison, 10 normal liver tissue samples (C1 to C10) showing no remarkable histological findings were also obtained from 10 patients without HCCs who were both HBs-Ag- and anti-HCV-negative. The patients comprised 7 men and 3 women with a mean age of 58.4 ± 9.7 years. Nine patients underwent partial hepatectomy for liver metastases of primary colon cancers, and 1 patient did so for liver metastases of gastrointestinal stromal tumor of the stomach.

In addition, for the comparison, 7 liver tissue samples (V1 to V7) were obtained from 7 patients who were positive for HBs-Ag or anti-HCV, but who had never developed HCCs. The patients comprised 4 men and 3 women with a mean age of 62.4 ± 5.2 years. Three patients underwent partial hepatectomy for liver metastases of primary colon or rectal cancers, and 1 patient did so for liver metastases of gastric cancer. Three patients underwent partial hepatectomy for cholangiocellular carcinomas.

As a validation cohort, 26 normal liver tissue samples (C11 to C36) showing no remarkable histological features were obtained from 26 patients without HCCs who were both HBs-Ag- and anti-HCV-negative. Twenty-four noncancerous liver tissue samples (N16 to N 39) and 25 primary HCCs (T20 to T44) were obtained from surgically resected specimens from 24 patients who underwent partial hepatectomy were added. The patients from whom C11 to C36 were obtained comprised 21 men and 5 women with a mean age of 59.9 ± 10.9 years. The patients with HCCs from whom N16 to N 39 and T20 to T44 were obtained comprised 22 men and 2 women with a mean age of 61.6 ± 11.4 years. Of the 24 patients with HCCs from whom N16 to N 39 and T20 to T44 were obtained, 5 were positive for HBs-Ag, 16 were positive for anti-HCV and 3 were negative for both. Histological examination of N16 to N 39 revealed findings compatible with chronic hepatitis and cirrhosis in 16 and 8 samples, respectively.

This study was approved by the Ethics Committee of the National Cancer Center, Tokyo, Japan.

BAMCA

High molecular weight DNA from fresh-frozen tissue samples was extracted using phenol-chloroform followed by dialysis. Because DNA methylation status is known to be organ specific, the reference DNA for analysis of the developmental stages of HCCs should be obtained from the liver and not from other organs or peripheral blood. Therefore, a mixture of normal liver tissue DNA obtained from 5 male patients (C37 to C41) and 5 female patients (C42 to C46) was used as a reference for analyses of male and female test DNA samples, respectively.

DNA methylation status was analyzed by BAMCA using a custom-made array (MCG Whole Genome Array-4500) harboring 4,361 BAC clones located throughout chromosomes 1 to 22 and X and Y,[19] as described previously.[16–18] Briefly, 5-μg aliquots of test or reference DNA were first digested with 100 units of methylation-sensitive restriction enzyme *Sma* I and subsequently with 20 units of methylation-insensitive *Xma* I. Adapters were ligated to *Xma* I-digested sticky ends, and polymerase chain reaction (PCR) was performed with an adapter primer set. Test and reference PCR products were labeled by random priming with Cy3- and Cy5-dCTP (GE Healthcare, Buckinghamshire, UK), respectively, and precipitated together with ethanol in the presence of Cot-I DNA. The mixture was applied to array slides and incubated at 43°C for 72 hr. Arrays were scanned with a GenePix Personal 4100A (Axon Instruments, Foster City, CA) and analyzed using GenePix Pro 5.0 imaging software (Axon Instruments) and Acue 2 software (Mitsui Knowledge Industry, Tokyo, Japan). The signal ratios were normalized in each sample to make the mean signal ratios of all BAC clones 1.0.

Statistics

Differences in the average number of BAC clones that showed DNA methylation alterations between groups of samples were analyzed using the Mann-Whitney *U* test or the Kruskal-Wallis test. Correlations between DNA methylation alterations in noncancerous liver tissue samples and the incidence of metachronous development and recurrence of HCCs were analyzed using the chi-squared test. Differences at $p < 0.05$ were considered significant. BAC clones whose signal ratios yielded by BAMCA were significantly different between groups of samples were identified by Wilcoxon test ($p < 0.01$). A support vector machine algorithm and a leave-one-out cross-validation were used to identify BAC clones by which the cumulative error rate for discrimination of sample groups became minimal. Two-dimensional hierarchical clustering analysis of noncancerous liver tissue samples and the BAC clones, and such analysis of HCCs and the BAC clones, were performed using the Expressionist software program (Gene Data, Basel, Switzerland). Survival curves of patient groups with HCCs were calculated by the Kaplan-Meier method, and the differences were compared by the log-rank test. The Cox proportional hazards multivariate model was used to examine the prognostic impact of DNA methylation status, histological differentiation, portal vein tumor thrombi, intrahepatic metastasis and multicentricity. Differences at $p < 0.05$ were considered significant.

Results

Genome-wide DNA methylation alterations during multistage hepatocarcinogenesis

Figures. 1*a* and 1*b* show examples of scanned array images and scattergrams of the signal ratios (test signal/reference signal), respectively, for normal liver tissue from a patient without HCC (Panel C), and both noncancerous liver tissue (Panel N) and cancerous tissue (Panel T) from a patient with HCC. In all normal liver tissue samples, the signal ratios of 97% of the BAC clones were between 0.67 and 1.5 (red bars in Fig. 1*b*). Therefore, in noncancerous liver tissue obtained from patients with HCCs and HCCs, DNA methylation status corresponding to a signal ratio of less than 0.67 and more than 1.5 was defined as DNA hypomethylation and DNA hypermethylation of each BAC clone compared with normal liver tissue, respectively.

In samples of noncancerous liver tissue obtained from patients with HCCs, many BAC clones showed DNA hypo- or hypermethylation (Panel N of Fig. 1*b*). In the learning cohort, all 9 patients (100%) showing DNA hypo- or hypermethylation on 70 or more than 70 BAC clones in their noncancerous liver tissue samples developed metachronous or recurrent HCCs after hepatectomy, whereas only 2 (30%) of the 6 patients showing DNA hypo- or hypermethylation on less than 70 BAC clones in their noncancerous liver tissue samples did so ($p = 0.0235$).

In HCCs themselves, more BAC clones showed DNA hypo- or hypermethylation, and the degree of DNA hypo- or hypermethylation, *i.e.*, deviation of the signal ratio from 0.67 or 1.5, was increased (Panel T of Fig. 1*b*) in comparison with noncancerous liver tissue obtained from patients with HCCs. The average numbers of BAC clones showing a signal ratio of less than 0.67 ($p = 0.0000063$) and more than 1.5 ($p = 0.00000052$) were increased significantly relative to normal liver tissue, to noncancerous liver tissue obtained from patients with HCCs, and to HCCs (Table I).

There were no significant differences in the number of BAC clones showing DNA hypo- or hypermethylation in samples of normal liver tissue obtained from male and female patients without HCCs (66.0 ± 30.1 and 98.7 ± 55.9, $p = 0.362$) and noncancerous liver tissue (111.2 ± 68.4 and 60.7 ± 46.9, $p = 0.279$) and cancerous tissue (521.5 ± 255.8 and 626.7 ± 329.0, $p = 0.539$) obtained from male and female patients with HCCs, respectively. Although there were no significant differences in the number of BAC clones showing DNA hypo- or hypermethylation between HBV- and HCV-positive patients with HCCs in both noncancerous liver tissue (108.3 ± 80.5 and 98.4 ± 60.0, $p = 1.000$) and cancerous tissue (475.6 ± 323.8 and 497.0 ± 247.8, $p = 0.689$), Wilcoxon test ($p < 0.01$) identified BAC clones in which DNA methylation status differed significantly between HBV- and

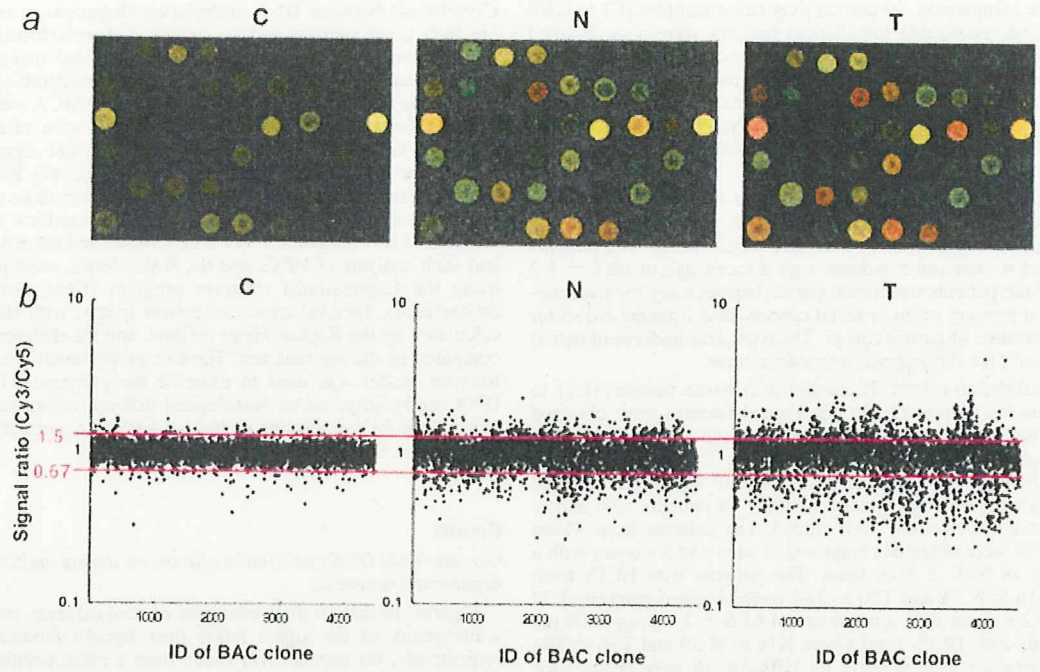

FIGURE 1 – Genome-wide DNA methylation alterations during multistage hepatocarcinogenesis. (*a*) Scanned array images yielded by BAMCA in normal liver tissue obtained from a patient without HCC (C) and noncancerous liver tissue (N) and cancerous tissue (T) obtained from a patient with HCC. (*b*) Scattergrams of the signal ratios yielded by BAMCA. In all C samples, the signal ratios of 97% of BAC clones were between 0.67 and 1.5 (red bars). In N and T, DNA methylation status corresponding to a signal ratio of less than 0.67 and more than 1.5 was defined as DNA hypomethylation and DNA hypermethylation on each BAC clone compared with C, respectively. Even in N, many BAC clones showed DNA hypo- or hypermethylation. In T, more BAC clones showed DNA hypo- or hypermethylation, and the degree of DNA hypo- or hypermethylation, *i.e.*, deviation of the signal ratio from 0.67 or 1.5 was increased in comparison with N.

TABLE I – GENOME-WIDE DNA METHYLATION ALTERATIONS DURING MULTISTAGE HEPATOCARCINOGENESIS

Tissue samples	Average number of BAC clones (mean ± SD)					
	Signal ratio <0.67 (DNA hypomethylation)	*p*	Signal ratio >1.5 (DNA hypermethylation)	*p*	Signal ratio <0.67 or >1.5(DNA hypo- or hypermethylation)	*p*
Normal liver tissue samples obtained from patient without HCCs (C, $n = 10$)	39.9 ± 20.8	0.0000063[1]	38.9 ± 24.9	0.00000052[1]	75.8 ± 39.3	0.00000061[1]
Noncancerous liver tissue samples obtained from patient with HCCs (N, $n = 15$)	61.2 ± 46.8	0.000102[2]	39.9 ± 27.3	0.0000026[2]	101.1 ± 66.5	0.0000065[2]
HCCs (T, $n = 19$)	278.9 ± 167.7	–	228.9 ± 125.7	–	507.8 ± 281.9	–

p values <0.05, which indicate significant differences.
[1]Kruskal-Wallis test among C, N and T.–[2]Mann-Whitney *U* test between N and T.

HCV-positive patients with HCCs in noncancerous liver tissue (18 BAC clones) and cancerous tissue (15 BAC clones), respectively.

DNA methylation profiles discriminating noncancerous liver tissue obtained from patients with HCCs from normal liver tissue

The above findings indicating accumulation of clinicopathologically significant genome-wide DNA methylation alterations in noncancerous liver tissue prompted us to estimate the degree of carcinogenetic risk based on DNA methylation profiles. Wilcoxon test ($p < 0.01$) revealed that the signal ratios of 512 BAC clones differed significantly between normal liver tissue samples and noncancerous liver tissue samples obtained from patients with HCCs. To omit potentially insignificant BAC clones associated only with inflammation and/or fibrosis and focus on BAC clones for which DNA methylation status was inherited by HCCs from the precancerous stage, we defined Groups I, II, III and IV. Group I: BAC clones in which the average signal ratio of noncancerous liver tissue obtained from patients with HCCs was higher than that of normal liver tissue and the average signal ratio of HCCs was even higher than that of noncancerous liver tissue obtained from patients with HCCs (41 BAC clones), Group II: BAC clones in which the average signal ratio of noncancerous liver tissue obtained from patients with HCCs was higher than that of normal liver tissue and the average signal ratio of HCCs did not differ from that of noncancerous liver tissue obtained from patients with HCCs (146 BAC clones), Group III: BAC clones in which the average signal ratio of noncancerous liver tissue obtained from patients with HCCs was lower than that of normal liver tissue and the average signal ratio of HCCs was even lower than that of noncancerous liver tissue obtained from patients with HCCs (40 BAC clones), and Group IV: BAC clones in which the average signal ratio of noncancerous liver tissue obtained from patients with HCCs was lower than that of normal liver tissue and the average